ENHANCEMENT OF VISIBLE-LIGHT-DRIVEN PHOTOCATALYTIC ACTIVITY OF TIO2/WO3 NANOCOMPOSITE FOR ORGANIC REMOVAL

YI YI ZAW

A Thesis Submitted to the Graduate School of Naresuan University
in Partial Fulfillment of the Requirements
for the Master of Engineering in (Environmental Engineering)
2019

Copyright by Naresuan University

YI YI ZAW

A Thesis Submitted to the Graduate School of Naresuan University
in Partial Fulfillment of the Requirements
for the Master of Engineering in (Environmental Engineering)
2019

Copyright by Naresuan University

Thesis entitled " ENHANCEMENT OF VISIBLE-LIGHT-DRIVEN PHOTOCATALYTIC ACTIVITY OF TiO2/WO3 NANOCOMPOSITE FOR ORGANIC REMOVAL "

By YI YI ZAW

has been approved by the Graduate School as partial fulfillment of the requirements for the Master of Engineering in Environmental Engineering of Naresuan University

Oral Defense Committee

..... Chair
(Assistant Professor Thotsaphon Threrujirapapong, Ph.D.)

..... Advisor
(Assistant Professor Wilawan Khanitchaidecha, Ph.D.)

..... Co Advisor
(Assistant Professor Duangdao Channei, Ph.D.)

..... Internal Examiner
(Assistant Professor Pajaree Thongsanit, Ph.D.)

Approved

.....
(Professor Paisarn Muneesawang, Ph.D.)

for Dean of the Graduate School

Title	ENHANCEMENT OF VISIBLE-LIGHT-DRIVEN PHOTOCATALYTIC ACTIVITY OF TIO2/WO3 NANOCOMPOSITE FOR ORGANIC REMOVAL
Author	YI YI ZAW
Advisor	Assistant Professor Wilawan Khanitchaidecha, Ph.D.
Co-Advisor	Assistant Professor Duangdao Channei, Ph.D.
Academic Paper	Thesis M.Eng. in Environmental Engineering, Naresuan University, 2019
Keywords	TiO2/WO3 nanocomposite photocatalysis process wastewater treatment organic removal

ABSTRACT

Water is importance to all living things. However, freshwater resources are limited and facing an increasing pressure from drought, flood, pollution, population growth, and competition from many uses (e.g., ecosystem protection, agriculture, energy production, and recreation). In the meanwhile, decrease in the quality of water resource from pollution and contamination (such as heavy metals, dyes, pesticides) by various types of discharge is a serious environmental problem in all over the world.

In order to overcome the future water scarcity, wastewater treatment is an effective solution to improve the wastewater quality and reuse it in any proposes. In many wastewater treatment methods, advanced oxidation processes (AOPs) have received increasing attention in research and development of wastewater treatment technologies in last decades. Among of the AOPs, photocatalysis process is considered as the greenest technology, due to high stability of photocatalyst and no toxic secondary pollutants formation.

Moreover, photocatalysis process is effective organic degradation, which is a common pollutant in the wastewater. Various photocatalysts can be used, however TiO_2 has been known as the most widely used photocatalyst. Due to its relatively wide band gap (~3.2eV), TiO_2 can be activated under strong light energy such as UV. This becomes an important operating cost of using photocatalysis process of TiO_2 for wastewater treatment and reuse. WO_3 is another photocatalyst, having a low band gap

value of 2.4–2.8 eV, and widely used for base material for biomarker detection and gas sensor. Therefore, a hybrid of TiO_2 and WO_3 as TiO_2/WO_3 composite is possible to enhance the photocatalytic activity as well as the properties of each TiO_2 and WO_3 photocatalyst.

In this work, TiO_2/WO_3 nanocomposite was synthesized by using hydrothermal method at various ratios of WO_3 from 0.01% to 0.3%. The physico-chemical properties of this nanocomposite were investigated by X-ray Diffraction (XRD), Transmission Electron Microscopy (TEM), and Brunauer–Emmett–Teller (BET) analytical instruments. Furthermore, the adsorption and photocatalytic degradation of methylene blue (MB) as a model organic pollutant were investigated, and then compared to pure TiO_2 and pure WO_3. The results showed that the increasing ratios of WO_3 can cause an enhancement of adsorption ability of TiO_2/WO_3 nanocomposite, and consequently increase MB photocatalytic degradation. Approximately 22% of MB was removed by adsorption and later degraded by photocatalytic degradation in 10 min with kinetic constant value (k) of 0.22 min^{-1}, when TiO_2/WO_3 0.01%wt. was used as photocatalyst. At the highest ratio of TiO_2/WO_3 0.3%wt., the high adsorption of 57% was found, while the k value of MB photocatalytic degradation was also high as 0.33 min^{-1}. This is because the improvement of photocatalyst properties including band gap energy (< 2.8 eV), specific surface area (> 105.6253 m^2/g), pore volume (> 0.2550 cm^3/g) and pore size (< 79.571 A°).

ACKNOWLEDGEMENTS

My deep gratitude goes first to my advisor Dr. Wilawan Khanitchaidecha for being an outstanding advisor. Her patience, enthusiastic instruction, constant encouragement, immense knowledge and guidance made my M.Eng. program and thesis successful.

My appreciation also extends to Dr. Duangdao Channei and Dr. Auppatham Nakaruk for their encouragement, suggestions, valuable knowledge on photocatalytic process, and useful comments throughout my research work.

I am grateful to the department of Civil Engineering as well as the Faculty of Engineering. Their help and assistance were critical for the successful completion of my Master program.

I would like to thank Naresuan University, Thailand International Cooperation Agency (TICA), Thailand Research Fund (TRF) and Office of the Higher Education Commission (CHE) for the financial support that allowed me to pursue my Master program at Naresuan University.

I also thank to my laboratory colleagues and friends, who helped and provided me a lot throughout my student life at Naresuan University.

YI YI ZAW

TABLE OF CONTENTS

Page

List of tables

Page

List of figures

Page

ABBREVIATION

TiO_2	=	Titanium dioxide
WO_3	=	Tungsten oxide
UV	=	Ultra violet
$^{\bullet}OH$	=	Hydroxylradical
TTIP	=	Titanium isopropoxide
MB	=	Methylene Blue
BET	=	Brunauer–Emmett–Teller
TEM	=	Transmission Electron Microscopy
XRD	=	X-Ray Diffraction
XPS	=	X-ray Photoelectron Spectroscopy

CHAPTER I

INTRODUCTION

Background

Water is major importance to all living things; in some organisms, up to 90% of their body weight derives from water. In the human body, up to 60% is water. The unique qualities and properties of water are what make it so essential and basic to life (Drinan & Spellman, 2012). Our earth is now facing many problems such as climate change and scarcities, and all of them result from human activity. Water scarcity is one of the largest challenges because safe drinking water is decreasing year by year. Nothing can live without water as well as human beings, so it is needed to keep clean water from decreasing from now on.

Wastewater treatment has been known as an effective solution to resolve the problem of water scarcity around the world. The presently common technologies used in wastewater treatment contain physical processes such as sedimentation, flocculation and coagulation, filtration, carbon adsorption, chemical oxidation processes (i.e., chlorination and ozonation) and biological processes (i.e., activated sludge, nitrification and denitrification). These wastewater treatment technologies have an extended history in large scale application and show usefulness in elimination of conventional (CDM Smith Inc. 2012).

Advanced oxidation processes (AOPs), well-defined as those technologies that use the hydroxyl radical ($^{\bullet}OH$) for oxidation, have received increasing attention in the research and advance of wastewater treatment technologies in the last decades. These processes have been applied effectively for the removal or degradation of toxic pollutants or used as pretreatment to convert recalcitrant pollutants into biodegradable compounds that can then be treated by conventional biological methods. The efficiency of AOPs depends on the generation of reactive free radicals, the most important of which is the hydroxyl radical ($^{\bullet}OH$) (Wang & Xu, 2012).

Among of the AOPs, photocatalysis is considered to be the better control of hydroxyl radical generation and toxic secondary pollutants formation compared to other processes. The photocatalysis is a kind of chemical method, which appears to be

quite favorable because of its simplicity, low cost, non-toxic, high degradation efficiency, and excellent stability. Semiconductor photocatalysis is a new method of wastewater treatment which was advanced in 1972. It has been received much consideration as a potential solution to the wastewater treatment and stop the deterioration of the environment (Jiang, et al., 2012).

Accordingly, semiconductors including TiO_2, WO_3, Bi_2WO_6, ZnO, and CdS etc. have been described to be used in water splitting to produce hydrogen or oxygen (Guo, et al., 2012). Noticeably, TiO_2 has proven to be a suitable candidate for photocatalytic applications. However, there are some weaknesses such as wide band gap of about 3.2 eV, fast recombination of electron (e^-)-hole (h^+) pairs. Many approaches have been accepted to improve the photocatalytic property of TiO_2 such as doping with metal or metal oxides, noble metal deposition and anion doping etc. The TiO_2 coupled with metal oxides shows better photocatalytic activity which is recognized to the split-up of charges. The tungsten oxide (WO_3), having low band gap values in the range of 2.4–2.8 eV, deeper valence band of +3.1 eV, 15 times more acidity than TiO_2 and good thermal stability, is suitable to couple with TiO_2. The lower conduction band (CB) position of WO_3 than that of TiO_2 assists the electron transfer from TiO_2 to WO_3 and the holes transfer in opposite direction. Therefore, better charge separation may be achieved. Earlier studies show that the enhanced photocatalytic activity of TiO_2/WO_3 is recognized to their high surface acidity, high surface area and reduction in the rate of recombination of e^--h+ pairs at the interface (Prabhu, et al., 2018).

The efficiency of the TiO_2/WO_3 for the photocatalytic applications can be enhanced by inhibiting the recombination of e^--h^+ pairs. The enhancement of the photocatalytic activity of TiO_2/WO_3 has been achieved by adopting several methods which include morphology control, semiconductor coupling, noble metal deposition, metal ion doping and formation of composites with graphene-related materials (eg. graphene oxide and/or reduced graphene oxide (rGO)). Among these methods, the formation of composites with graphene has attracted great attention because of the special properties such as high surface area, high electrical conductivity, high carrier movement and efficient electron (e^-) collection and transport (Prabhu, et al., 2018).

Hence, this work aims to synthesis TiO_2/WO_3 nanocomposite by hydrothermal method. The properties and characteristics of these nanocomposites are examined by X-ray Diffraction (XRD), X-ray Photoelectron Spectroscopy (XPS), Transmission Electron Microscopy (TEM), and Brunauer–Emmett–Teller (BET) method. The photocatalytic activity of TiO_2/WO_3 nanocomposite was investigated via the degradation of methylene blue (MB) as sample pollutant.

Objectives of research

1. To synthesize and characterize TiO_2/WO_3 nanocomposite
2. To evaluate the adsorption and photocatalytic activity of TiO_2/WO_3 nanocomposite for organic pollutant removal

Scope of research

TiO_2/WO_3 nanocomposites are synthesized by hydrothermal method. This work focus on the enhancement of photocatalytic activity of TiO_2/WO_3 nanocomposite for wastewater treatment.

CHAPTER II

LITERATURE REVIEW

Current status of water resource

Water is essential resource and basic to life for all living things. Water resource is decreasing because of many factors such as climate change, over-exploitation, and pollution. Besides, higher water demand comes from increasing population, rapid growth of economic and industrial sector. A major driver of water demand is population pressure and this issue is today's scenarios of future water stress. Higher population density leads to the higher demand for water use.

Even in the absence of significant pollution pressure, water demand is likely to increase with economic and industrial sector. Factors such as increasing population, rapid growth of economic development and industrial sector on water resource leads water scarcity and significant impacts on people and the environment (Böhmelt, et al., 2014). Between 1950 and 1990 the number of world cities with a population greater than 1 million increased from 78 to 290 and is expected to rise to 600 by 2025 (Hinrichsen & Tacio, 2002). The links between human activity and water resource are illustrated in Figure 1. According to United Nation Water Organization (UN-Water), water demand is increasing three times as fast as the world's population growth rate (Sridhar, 2013).

The world's freshwater resources such as the rainfall that is kept in the soil and then evaporates or is combined in plants and organisms is the main source of water for natural ecosystems and renewable surface water runoff and groundwater recharge is the major source for human withdrawals and focus of water resource management (Cosgrove & Rijsberman, 2014).

Water scarcity has become one of the most interesting issues of the world. According to WHO (2003), 1.2 billion people lack access to safe and affordable water for their domestic use. More and more countries are facing water stress and scarcity as their populations raise, urbanization accelerates, and water consumption increases. To consider whether the water needs of all human users and the environment are safe and

conversely whether water is limited or not, needs an analysis of how much water is available or can be made available.

Two-thirds of the global populations (4.0 billion people) live under conditions of severe water scarcity at least 1 month of the year. Approximately half of those people live in India and China. Half a billion people in the world face severe water shortage all year round. Large water consumption relative to water availability results in reduced river flows, mostly during the dry period, and decreasing lake water and groundwater levels. Businesses depending on water in their processes or supply chain also face increasing risks of water scarcity (Rijsberman, 2006; Mekonnen & Hoekstra, 2016).

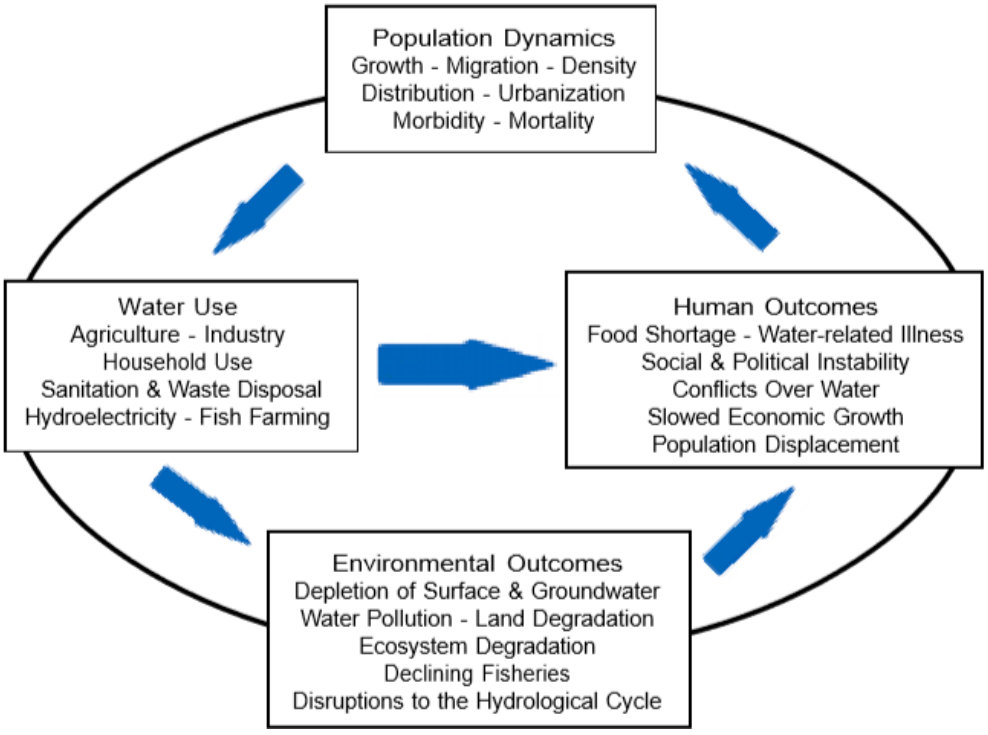

Figure 1 Links between human activity and water resource

Source: Hinrichsen, & Tacio, 2000

Pollutants in wastewater

1. **Organic compound**

There are several contaminants in wastewater, with organic pollutants live the major role. Many kinds of organic compounds, such as PCBs, pesticides, herbicides, phenols, polycylic aromatic hydrocarbons (PAHs), are included in the wastewater. The wastewater of the farmland may contain high concentration of pesticides or herbicides, the wastewater of the chemical industry may contain various heterogeneity compounds, such as polychlorobiphenyls (PCBs), the wastewater discharged by the food industry contains complex organic pollutants with high concentration of SS and BOD; and the municipal sewage contains different type of organic pollutants, such as oil, food, some dissolved organics and some surfactants. These organic pollutants in water can harm the environment and besides pose health threats for humans (Zheng, et al., 2013; Deblonde, et al., 2011).

2. **Total dissolved solids**

Total Dissolved Solids (TDS) are solids in water that can go through a filter. TDS characterizes the total concentration of dissolved substances in water. This material can contain carbonate, bicarbonate, chloride, sulfate, phosphate, nitrate, calcium, magnesium, sodium, organic ions, and other ions. A certain level of these ions in water is needed for aquatic life. However, if TDS concentrations are too high or too low, the growing of many aquatic lives can be limited, and death may happen. TDS is used to estimate the quality of drinking water, because it characterizes the amount of ions in the water. High TDS in water often has a bad taste and/or high water hardness, and could result in a laxative effect. High concentrations of TDS in water body may also decrease water clarity, contribute to a decrease in photosynthesis, combine with toxic compounds and heavy metals, and cause an increase in water temperature. The large source of TDS can form such as steel industry, pharmaceutical manufacturing, mining operations, oil and gas extraction, some power plants, landfills, food processing facilities, and others (Semerjian & Ayoub, 2003; Wilson, et al., 2014).

3. Nutrients

In the process of a wastewater, nutrients are an important component. Specifically, the two macro-nutrients nitrogen and phosphorus are the basic constituents for the growth and reproduction of living organisms. However, human activities are affecting their natural cycles and causing excessive dumping into the surface and groundwater systems. Higher concentrations of nitrogen and phosphorus-based nutrients in water resources lead to eutrophication, reduction in sunlight, lower dissolved oxygen levels, changing rates of plant growth, reproduction patterns, and overall deterioration of water quality. Economically, this pollution can impact the fishing industry, recreational businesses, property values, and tourism. Also, using nutrient-polluted lakes or rivers as potable water sources may result in excess nitrates in drinking water, production of disinfection by-products, and associated health effects (Ambulkar, 2017; Gray, 2017).

4. Color

Dyes are colored substance that are used for imparting color to various substrates including paper, leather, drugs, cosmetics, waxes, plastics and textile materials. Wastewater discharges from industrial containing dyes cause serious environmental problems. Sources of industrial wastewater are like cement industries, pharmaceutical industries, food industries, textile industries, pulp paper industries, rubber industries, color photography Leather industries, cosmetics industries, plastic industries, organic compost and other industries used a large variety of chemical treatments and dyes has resulted in a public health threat created by pollution. Color in the effluent is one of the most noticeable indicators of water pollution and the discharge of highly colored synthetic dye effluents is very unpleasing and can damages the receiving water body by hindering the penetration of light (Gonawala & Mehta, 2014).

5. Metals

Heavy metals are one of the most persistent pollutants in wastewater. The discharge of high amounts of heavy metals into water bodies leads to numerous environmental and health impacts. The exposure of humans to heavy metals can occur

through a variety of ways, which include inhalation, vaporization and ingestion through dust, food and drink. Some harmful effects of heavy metals to aquatic environments include death of aquatic life, algal blooms, environment damage from sedimentation, increased water flow, and other short and long term toxicity from chemical contaminants. The effects on animals include reduced growth and development, cancer, organ damage, nervous system damage and death (Akpor, et al., 2014; Hezbullah, et al., 2016).

6. Bacteria

Microbial pathogens are among the major health problems related with water and wastewater. These pathogenic microorganisms cause several aquatic pollutions and diseases like bacterial. The major groups of pathogens that are of significance to wastewater are bacteria, viruses, fungi or protozoa. Among them bacteria are the most common pathogens in water, gain entrance into water mostly through fecal contamination. Bacterial pathogens cause typhoid, paratyphoid and other type diseases. Several types of bacteria can enter your body through polluted food or water and cause diarrhea in patient. (Cabral, 2010; Olaolu, et al., 2014).

Wastewater treatment and reclamation technology

Wastewater reuse is an idea that is rapidly achievement popularity in wastewater treatment. While conditions may dictate the necessary of wastewater reuse, now, generally, water reclamation (treatment or processing of wastewater to make it reusable) and reuse is achieved with increasing regularity. Wastewater is reused worldwide for agriculture, industry, drinking water, non-potable domestic uses, landscape irrigation, recreation, and groundwater recharge Wastewater reuse provides many benefits, and discharge can be reused easily for numerous purposes. Reuse offers an alternative disposal outlet that can accept a lower level of treatment, thus protecting delicate ecosystems and offsetting costs related with advanced treatment to meet discharge waste regulations. Wastewater can be reused to enhance or create recreational facilities; industrial water supplies, groundwater recharge, and for direct reuse for potable water supplies (Drinan & Spellman, 2012). An overview of worldwide wastewater reuse shared by applications is presented in Table 1.

Table 1 Global wastewater reuse for various applications

Reused water applications	Percentage (%)
Agricultural irrigation	32%
Landscape irrigation	20%
Industrial applications	19.3%
Non-potable urban supply	8.3%
Environmental enhancements	8%
Recreational applications	6.4%
Indirect potable supply	2.3%
Groundwater recharge	2.1%
Other	1.5%

Source: CDM Smith Inc. 2012

1. **Reverse osmosis (RO)**

Reverse osmosis purification is the most innovative and the best purification process used to purify water. RO purification process is highly capable of removing all the dissolved impurities the drinking water. If the TDS level of the water purifier is high then RO water purifier is the most suitable purifier to choose. It works on the principle of Reverse osmosis where a semi-permeable membrane is used to filter out even the minute impurities which cannot be seen with naked eyes. It is the only process that can remove even heavy metals and all dissolved chemicals from the drinking water. During RO purification, water is allowed to pass through the membrane under high pressure leaving behind all the impurities and provides pure water to drink. Process of reverse osmosis is illustrated in Figure 2 (Baker, 2012; Noble & Stern, 1995).

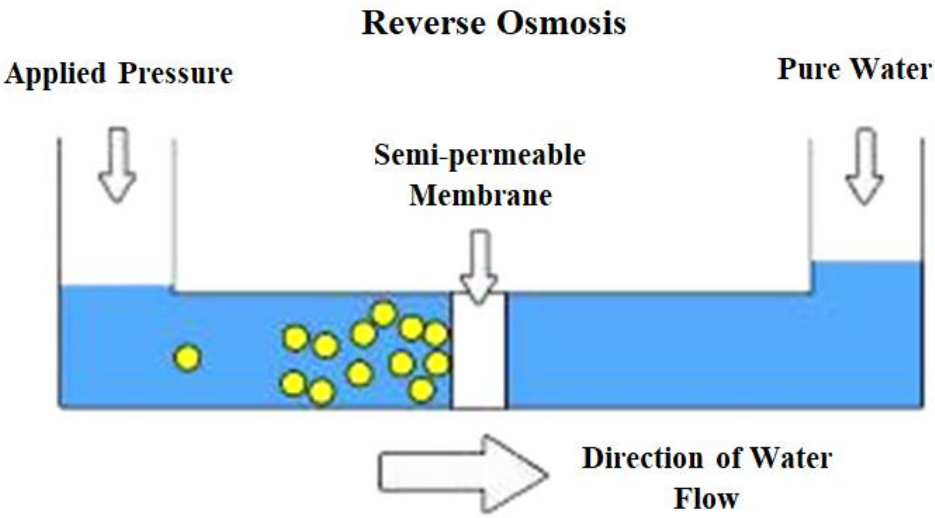

Figure 2 Purification process of reverse osmosis (RO)

2. Ultrafiltration (UF)

Ultrafiltration purification process is required in the purification of the water that contains low TDS level. A semi-permeable membrane is used in it, which the process is similar to RO process but membrane has comparatively large pore size then RO membrane. The membrane allows only those particles to pass through it which is smaller than pore size. Unlike UV process, Ultrafiltration process not only kills the microorganism but also flushes them out from the drinking water and does not require any further purification. Purification process of ultrafiltration (UF) is presented in Figure 3 (Noble & Stern, 1995; Afzali, et al., 2018).

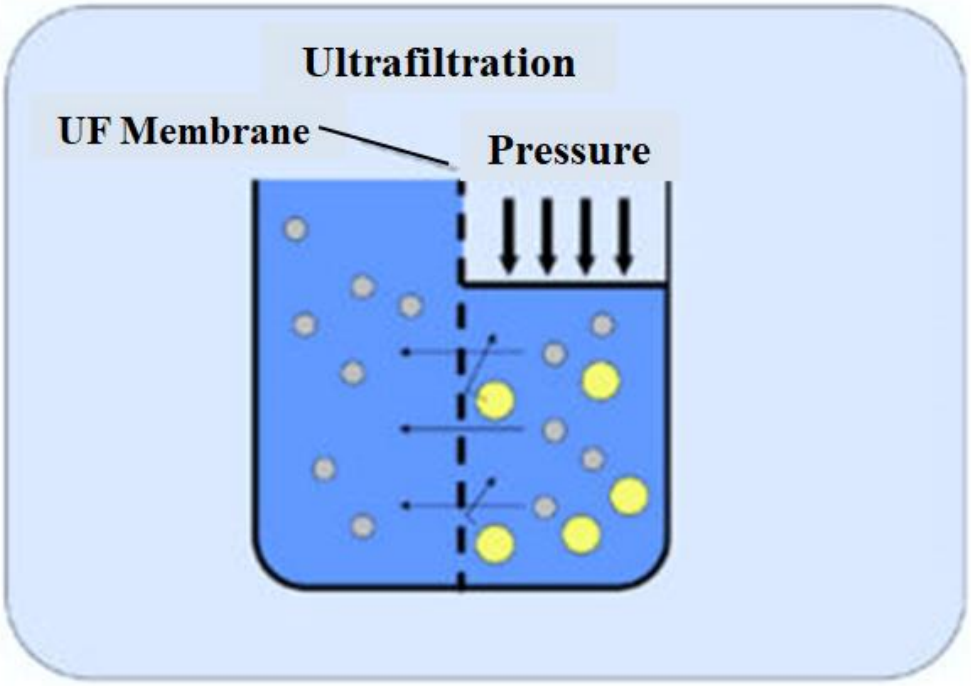

Figure 3 Purification process of ultrafiltration (UF)

3. Nanofiltration (NF)

Nanofiltration (NF) is a medium to high pressure-driven membrane filtration process. NF is a unique filtration process in-between ultrafiltration and reverse osmosis intended to attain highly specific separation of low molecular weight compounds such as minerals and salts from complex process streams. NF can also be used to treat all kinds of water including ground, surface, and wastewater or used as a pretreatment for purification. Typical applications include de-ashing of dairy and food products, recovery of hydrolyzed proteins, concentration of sugars and purification of soluble dyes and pigments (Hilal, et al., 2004; Afzali, et al., 2018).

4. Microfiltration (MF)

Microfiltration (MF) is a low pressure-driven membrane filtration process. The MF membrane is the most open membrane of the four membrane technologies. MF is used for separating large molecular weight suspended or colloidal compounds from dissolved solids. The element such as bacteria and suspended solids can be removed through microfiltration. The different pore sizes of different membranes

allow for different elements allowed to be passed through, giving ultimate precision to treating wastewater issue correctly and safely for the environment. Each filtration process has the same procedure, water passes through a semipermeable membrane, and depending on the pore size certain elements are removed whilst others pass through. Principles of the four main membrane filtration technologies as depicted in Figure 4 (Noble & Stern, 1995; Afzali, et al., 2018).

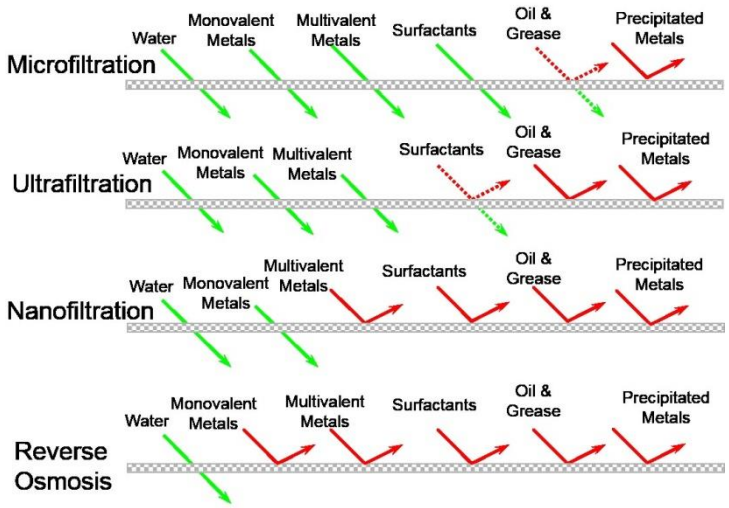

Figure 4 Principles of membrane filtration technologies

Advanced oxidation processes (AOPs)

In recent years, AOPs have been widely used in water treatment for its great potential and significant advantages. Among the innovative wastewater treatment technologies, advanced oxidation processes played an important part because of its advantages such as the ability of complete oxidation, high degradation efficiency, and the mineralization of pollutants without secondary pollution (Lei, et al., 2018). Advanced oxidation processes (AOPs) are the application of hydroxyl radicals ($OH^{\bullet}$) to oxidize organic compounds to form carbon dioxide (CO_2) and water (H_2O) as final products (Mascolo, et al., 2007; De la Cruz, et al., 2013). In waste-water treatment, AOPs usually refers as specific subsets of chemical processes that include O_3, H_2O_2 and/or UV light. However, AOPs could also be used to refer to a more general group of processes (Chan, et al., 2011). Additionally, AOPs can be operated under normal

condition (room temperature and atmospheric pressure) (Hawari, et al., 2015). A comparison of standard potential of some oxidants is shown in Table 2. As brief in Table 3, a large number of AOPs has been advanced, including non-photochemical and photochemical methods. The AOPs are effectively applied mainly for the treatment of wastewaters, but they are also used in various fields including groundwater treatment, soil remediation, municipal wastewater sludge conditioning, besides odor and taste removal from drinking water (Sirés, et al., 2014).

Table 2 Standard potential of oxidizing species

Oxidizing agent	Standard potential (V)
Oxygen (molecular)	1.23
Chlorine dioxide	1.27
Chlorine	1.36
Ozone	2.08
Oxygen (atomic)	2.42
Hydroxyl radicals	2.80
Fluorine	3.06
Positively charged hole on TiO_2	3.2

Source: Sirés, Ignasi, et al. 2014

Table 3 Main AOPs and related reactions involving the production of •OH

	Reactions
Dark AOPs	
Ozone at elevated pH	$3O_3+OH^-+H^+ \rightarrow 2^{\bullet}OH+4O_2$
Ozone+hydrogen peroxide	$2O_3+H_2O_2 \rightarrow 2^{\bullet}OH+3O_2$
Ozone+catalyst	$O_3+Fe_2^{+}+H_2O \rightarrow Fe_3^{+}+OH^-+^{\bullet}OH+O_2$
Fenton	$Fe_2^{+}+H_2O_2 \rightarrow Fe_3^{+}+OH^-+^{\bullet}OH$
Photo-assisted AOPs	
Ozone/UV	$O_3+H_2O+h\nu \rightarrow O_2+H_2O_2$

	Reactions
Hydrogen peroxide/UV	$H_2O_2+h\nu \rightarrow 2^{\bullet}OH$
Ozone/H_2O_2/UV	The addition of H_2O_2 to the O_3/UV process accelerates the decomposition of ozone, which results in an increased rate of $^{\bullet}OH$ generation
Photo-Fenton	$Fe_2^{+}+H_2O_2+h\nu \rightarrow Fe_3^{+}+OH^{-}+^{\bullet}OH$
	$Fe(OH)_2^{+}+h\nu \rightarrow Fe_2^{+}+^{\bullet}OH$
	$Fe(OOCR)_2^{+}+h\nu \rightarrow Fe_2^{+}+CO_2+R^{\bullet}$
Heterogeneous photocatalysis (TiO_2/UV)	$TiO_2+h\nu \rightarrow TiO_2(e^{-}+h^{+})$
	$h^{+}+H_2O \rightarrow {}^{\bullet}OH+H^{+}$
	$e^{-}+O_2 \rightarrow O_2^{-\bullet}$

Source: Sirés, Ignasi, et al. 2014

Photocatalysis process

Photocatalysis is an attractive technology that enables a wide diversity of applications, such as chemical synthesis, environmental technology, medicine, degradation of organics and dyes, and fuel generation through water splitting and carbon dioxide reduction (Van Gerven, et al., 2007). Photocatalysis is a kind of chemical method, which performs to be favorable because of its simplicity, low cost, nontoxic, high degradation efficiency, and excellent stability. Semiconductor photocatalysis is a new method of sewage treatment which was advanced in 1972. It has been received much consideration as a potential solution to the wastewater treatment and stop the deterioration of the environment (Jiang, et al., 2012).

In all photocatalytic processes, the foundation is the generation of electron^{-}/hole^{+} pairs in the photocatalyst through the adsorption of photons, where a photon adsorbed by photocatalysis promotes an electron from the valence band to the conduction band, leaving a positive hole in the valence band, as shown in Figure 5. Nanocomposites used for photocatalytic processes include TiO_2, ZnO, WO_3, Fe_2O_3, Al $_2O_3$, ZnS, and CdS, or coupled nanocomposites, such as CuO-SnO_2, TiO_2/WO_3, and TiO_2-SiO_2 (Wei, et al., 2013).

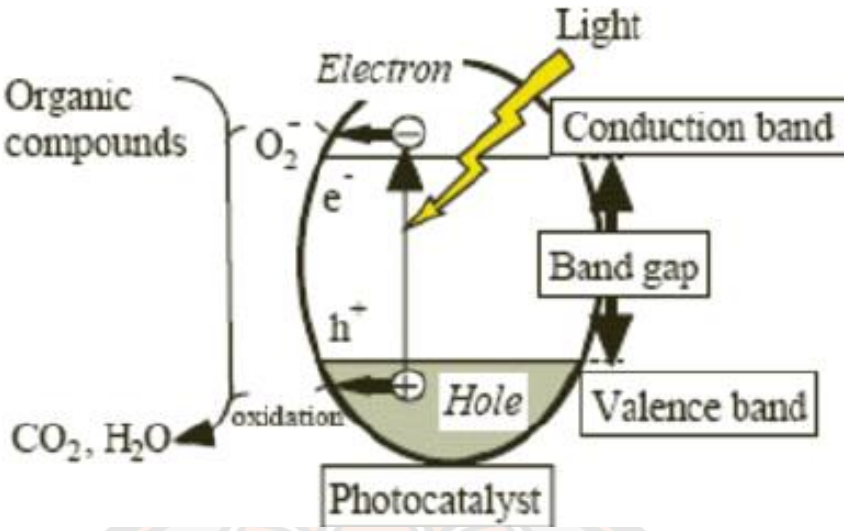

Figure 5 Photocatalytic process of organic compounds degradation

Source: Wei, et al., 2013

Other criteria to be considered when choosing an ideal water purification photocatalyst are: (a) thermodynamically stable in the presence of water; (b) the energy level of the valance band edge being well below the chemical potential of O_2/H_2O to prevent the corrosion of photocatalysts and maintain a high oxidation potential in the reaction; (c) low cost for synthesis; and (d) the bandgap of the photocatalyst being as low as possible in addition (Zhang, et al., 2009).

Many semiconductors have been studied intensively for the environmental cleaning. Bandgap energies of common catalyst are given in Table 4 (Thiruvenkatachari, et al., 2008).

Table 4 Bandgap energies of common semiconductors

Semiconductors	Bandgap energy (eV)	Semiconductors	Bandgap energy (eV)
Diamond	5.4	WO_3	2.76
CdS	2.42	Si	1.17
ZnS	3.6	Ge	0.744

Semiconductors	Bandgap energy (eV)	Semiconductors	Bandgap energy (eV)
ZnO	3.436	Fe_2O_3	2.3
TiO_2	3.03	PbS	0.286
CdS	2.582	PbSe	0.165
SnO_2	3.54	ZrO_2	3.87
CdSe	1.7	Cu_2O	2.172

1. Titanium dioxide (TiO_2) catalyst

As mentioned in the above, there are many different semiconductors which are used in photocatalytic reaction. Among many semiconductor photocatalysts, titanium dioxide is the most common used photocatalyst because of its high activity, large stability to light illumination, low price, nontoxicity and thermal resistance (Thiruvenkatachari, et al., 2008). TiO_2 is initiated by the absorption of a photon with energy equal to, or greater than the band gap of the semiconductor (3.2 eV for anatase), producing electron-hole (e-/h+) pairs, by the following equation (Jiang, et al., 2012).

$$TiO_2 \xrightarrow{hv} e^-_{cb}\,(TiO_2) + h^+_{vb}\,(TiO_2)$$

Where, cb is conduction band and vb is the valence band

1.1 Structure and properties

Titanium dioxide has different crystalline forms. The most common forms are anatase and rutile. The third crystalline form is brookite, which is uncommon and unstable. Both anatase and rutile have a tetragonal structure, in which the octahedron share vertices at planes and share edges at planes, respectively. There are three main types of the polymorphs of TiO_2: anatase, rutile and brookite as shown in Figure 6 (Pelaez, et al., 2012). Meanwhile, brookite has an orthorhombic structure as a result of the octahedron sharing of both edges and vertices.

Among of these polymorphs of titanium dioxide, anatase is the most stable form and can be converted to rutile by heating to temperatures ~ 600ºC. In the

photocatalysis applications, it is known that, anatase is more efficient than rutile, having an open structure compared with rutile. In general, brookite is relatively unstable and difficult to synthesize in pure form compared to anatase and rutile. Therefore, most of investigations into titanium dioxide are focused on anatase and rutile (Pelaez, et al., 2012; Luís, et al., 2011; Zhang, et al., 2009). The characteristics of these three structures are summarized in Table 5 (Pelaez, et al., 2012; Ola & Maroto-Valer, 2015).

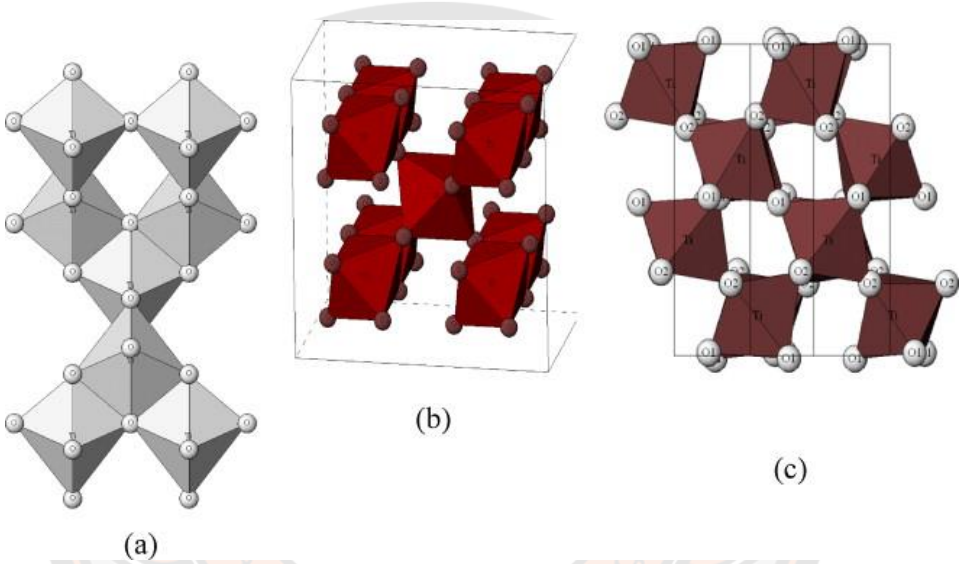

Figure 6 Crystalline structures of TiO_2 (a) anatase, (b) rutile, (c) brookite

Source: Pelaez, et al., 2012

Table 5 Significant properties of different TiO_2 phases

Properties	Anatase	Rutile	Brookite
Molecular weight (g/mol)	79.88	79.88	79.88
Melting point (°C)	1825	1825	Turning into rutile
Boiling point (°C)	2500–3000	2500–3000	-
Light absorption (nm)	<390	<415	-

Properties	Anatase	Rutile	Brookite
Refractive index	2.55	2.75	2.81
Dielectric constant	31	114	78
Crystal structure	Tetragonal	Tetragonal	Orthorhombic
Lattice constants (Å)	a = 3.78	a = 4.59	a = 9.16
	c = 9.52	c = 2.96	b = 5.43
			c = 5.14
Density (g/cm^3)	3.79	4.13	4.13

Anatase is stable at low temperature and has small grain sizes resulting higher surface areas and low surface energy. Anatase is a wide band gap semiconductor of 3.2 eV and can active only under UV. Rutile is more stable than Anatase and has lower band gap semiconductor of 3.0 eV but large grain sizes and high electron-hole recombination rate are disadvantage of Rutile phase (Yuangpho, et al., 2015). Due to the relatively large band gap, titanium dioxide is opaque to UV light and transparent to visible light. Thus, it has been used as a material for UV filtering, UV protection cosmetics and other products (Zhang, et al., 2009). The position of oxygen ions on the exposed crystal surface of anatase displays a triangular arrangement, allowing effective absorption of organics. On the other hand, this favorable structure arrangement is not available for rutile structure. For that reasons, anatase has higher photocatalytic activity than rutile (Ollis & Al-Ekabi, 1993; Smyth & Bish, 1998). The effect of particle size on the photocatalytic activity can be interpreted in terms of surface area. Thus the smaller the particle size, the larger the surface area and higher the expected activity (Thiruvenkatachari, et al., 2008).

1.2 Synthesis methods

There are various technologies that have been developed to synthesize TiO_2 particles such as sol–gel method, flame or aerosol process, precipitation, thermal decomposition reactions, hydrothermal method, and microwave assisted method

(Zhang, et al., 2009; Le, et al., 2012). In this work, the most common methods of nano sized TiO_2 synthesis including sol–gel, precipitation and hydrothermal methods are briefly introduced (Zhang, et al., 2009).

1.2.1 Sol-gel method

Sol-gel method is a wet chemical process to synthesize nanomaterials from a liquid phase. The precursors used in sol-gel method can be inorganic or metal-organic compounds. The most commonly applied precursors are metal alkoxides [$M(OR)_n$], in which R is an alkyl, inorganic salt, or organic salt. The overall reaction can be represented as follows (Zhang, et al., 2009):

Hydrolysis: $MOR + H_2O \leftrightarrow TiOH + ROH$

Condensation: $MOR + HOM \leftrightarrow MOM + ROH$ (alcoxolation)

$MOH + HOM \leftrightarrow MOM + H_2O$ (oxolation)

$MOH_2 + MOR \leftrightarrow M(OH)M + ROH$ (olation)

1.2.2 Hydrothermal method

Hydrothermal method is a widely used method to synthesize titanium dioxide. Hydrothermal method can be used to heat a solution to temperatures well above its boiling point and water is used as the solvent. By comparing with other methods, hydrothermal method has many advantages such as equipment and processes are very simple and it is easy to control the reaction conditions. But this synthesis method needs Telfon-lined stainless-steel autoclave.

1.2.3 Precipitation method

Precipitation is one of the oldest methods and most conventional to synthesize nanocomposite. In precipitation method, the precursors are dissolved in a solvent, such as water and base solution such as sodium hydroxide or ammonium hydroxide is added to promote the precipitation. In the precipitation method, the precipitates are filtered, dried and then it requires to treat high temperature as a calcination stage to develop crystalline structure.

1.3 Applications

TiO_2 photocatalysis can almost degrade all organic pollutants. Many kinds of difficultly degradable organic compounds can be degraded by TiO_2 photocatalytic technology and photocatalytic degradation of TiO_2 in wastewater treatment are shown in Table 6. The TiO_2 photocatalysis has not only used in wastewater treatment but

also applied in various applications such as air purification, electric appliance, side mirror for automobile, printing, self-cleaning and self-sterilizing as summarized in Figure 7 (Lee & Park, 2013).

Table 6 TiO_2 photocatalytic degradation of organic pollutants in wastewater treatment

Pollutant	Catalyst	Ref.
Methyl orange	Y-TiO_2-HPW	Yajun, et al., 2011
Alkaline red dye	TiO_2-Fenton	Khataee, et al., 2011
Rhodamine 6G	TiO_2	Asiri, et al., 2011
MB (50 mg/L)	TiO_2	Le, et al, 2012
Phenol	TiO_2	Gao, et al., 2014
Phenol	Degussa P-25	Zainudin, et al., 2010
Malathion pesticide	TiO_2	Ramos-Delgado, et al., 2013
4-chlorophenol	Degussa P-25	Naeem & Ouyang, 2013

Photocatalysis of TiO_2 can also be used in other environmental application. Photocatalysis of TiO_2 was found to be effective against a number of indoor air pollutants including inorganic gases such as NO and CO, VOCs such as benzene, toluene, and xylenes. There is also much attention in the use of TiO_2 coatings as self-cleaning surfaces that also show antibacterial properties and can efficiently kill bacteria (Stefanov, 2015). Due to the antibacterial ability, the photocatalysis of TiO_2 was effective for pharmaceutical and food industries (Skorb, et al., 2008). Another application of TiO_2 photocatalysis was offset printing and is used to print newspapers and magazines by an offset printing plate (Nakata & Fujishima, 2012).

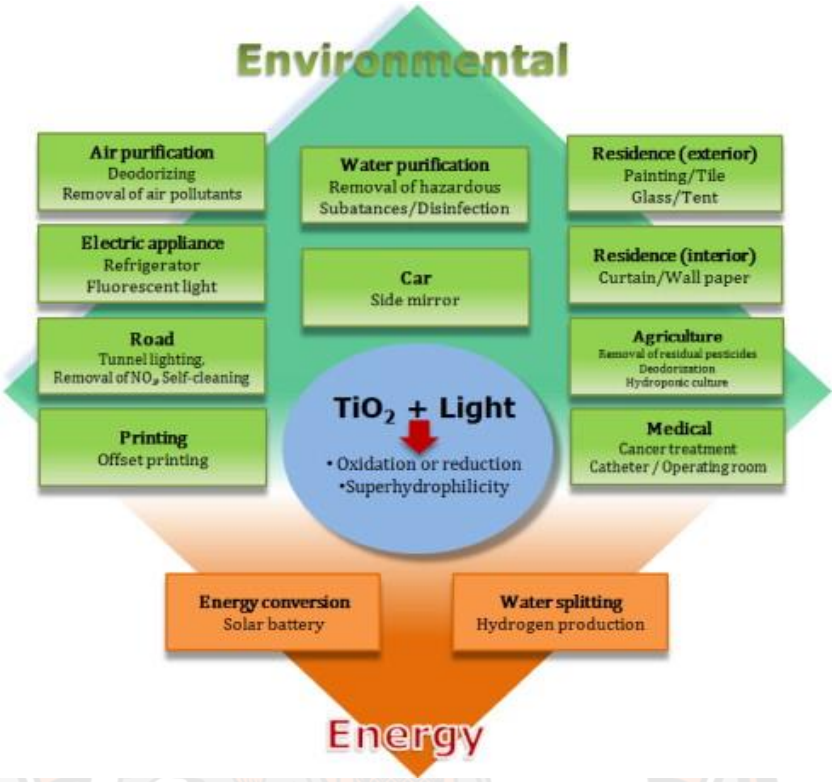

Figure 7 Applications of TiO_2 photocatalyst

Source: Lee & Park, 2013

2. Tungsten oxide (WO_3)

In recent years, nanostructured tungsten oxide (WO_3), as one of the n type semiconductors with a band gap of 2.8 eV, has received a lot of interests in photocatalysis because of their great potential applications as its strong adsorption, high photo-activity, excellent electron transport properties and stable physicochemical properties. Under the irradiation of visible light, photo induced electrons and holes can be formed in the conduction band and valence band respectively (Guo, et al., 2012; Mehmood, et al., 2017). The reaction mechanism for photocatalytic degradation is as under (Tahir, et al., 2017).

$$WO_3 + h\nu \rightarrow h^+(VB) + e^-(CB)$$

$$e^- + O_2 \rightarrow {}^{\bullet}O_2^-$$

$h^+ + OH^- \rightarrow {}^{\bullet}OH$

$O_2^- +$ dyes (pollutant) → Degradation of dyes

OH + dyes (pollutant) → Degradation of dyes

2.1 Structure and properties

Tungsten oxide exhibits a cubic perovskite like structure based on the corner sharing of regular octahedral with the oxygen atoms at the corner and the tungsten atoms at the center of each octahedron. The crystal structure of tungsten oxide is dependent on temperature. The most common structure of WO_3 is monoclinic form. Structural order and morphology of WO_3 can be affected by the physical properties of a material. The enhancement of materials properties needs a closer inspection of preparation conditions. The crystal structure of monoclinic WO_3 as presented in Figure 8 (Rao, 2013).

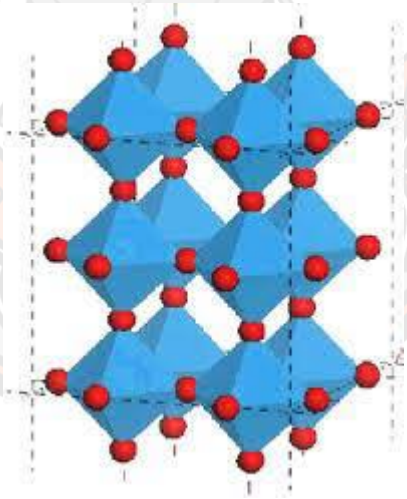

Figure 8 Crystalline structures of WO_3

Source: Rao, 2013

2.2 Synthesis methods

As above mentioned tungsten oxide (WO_3) is an effective photocatalyst and can be deposited by using various techniques such as hydrothermal method,

precipitation method, solvothermal method, and sol–gel method. However, the present work only provides precipitation method to synthetic WO_3. Precipitation is one of the oldest methods to synthesize nanoparticles.

2.3 Applications

Tungsten oxide is used for many purposes in everyday life such as inorganic and organic synthesis, photolysis of water into hydrogen and oxygen evolution, the photocatalytic reduction of metal ions, photocatalytic degradation of organic pollutants, air purification, and self-cleaning, etc. Some applications of tungsten oxide are shown in Figure 9 (Tahir, et al., 2017).

WO_3-based photocatalyst can be applied for other applications. Tungsten oxide photocatalyst can be used for inorganic and organic synthesis, photolysis of water into hydrogen and oxygen evolution, the photocatalytic reduction of metal ions (such as heavy metal of chromium, mercury, lead etc.), photocatalytic degradation of organic pollutants (such as formaldehyde), self-cleaning (such as used in the automotive side mirrors), anti-bacterial and antiseptic (Tahir, et al., 2017).

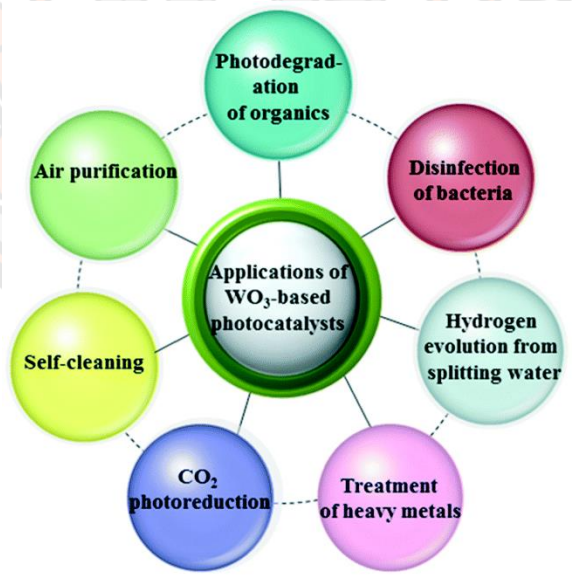

Figure 9 Applications of tungsten oxide photocatalyst

Source: Tahir, et al., 2017

3. TiO_2/WO_3 nanocomposite

According to the literature reviews and results from many researches, TiO_2 has proven to be a well-known candidate for photocatalytic applications. However, there are some disadvantages such as wide band gap about 3.2eV makes it a poor absorber of solar radiation. Another disadvantage is fast recombination rate of electron and hole. The charge carriers cannot reach the surface and react with the adsorbed organic molecules to initiate the degradation process during the short life-time. So, many approaches have been accepted to improve the photocatalytic property of TiO_2 such as doping with metal or metal oxides (Prabhu, et al., 2018; Gaikwad, et al., 2016).

As mentioned in the above the lower conduction band (CB) position of WO_3 than that of TiO_2 assists the electron transfer from TiO_2 to WO_3 and the holes transfer in opposite direction. Therefore, better charge separation may be achieved. Earlier studies show that the enhanced photocatalytic activity of TiO_2/WO_3 is recognized to their high surface acidity, high surface area and reduction in the rate of recombination of e^--h+ pairs at the interface (Prabhu, et al., 2018). Mechanistic illustration of photocatalytic processes of TiO_2/WO_3 is presented in Figure 10.

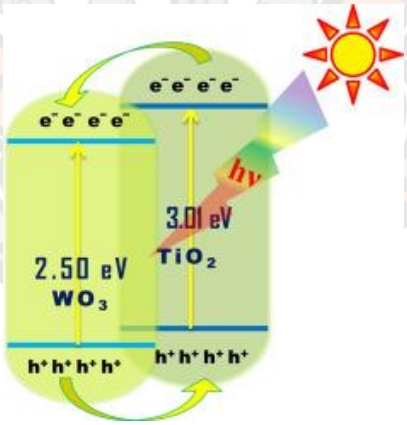

Figure 10 Mechanistic illustration of photocatalytic processes of TiO_2/WO_3

Source: Prabhu, et al., 2018

Previous studies on TiO_2/WO_3 and TiO_2/W photocataysts

The use of particulate or colloidal semiconductors in solutions has widely been studied for the photocatalytic oxidation of organic waste and pollutants in water

was introduced by the work of Fujishima and Honda in 1972. As introduced, among various semiconductor photocatalysts, TiO_2 has been proven as the most effective and useful photocatalyst. To improve photocatalytic activity of TiO_2 for wide range applications, most studies have been reported that the coupling of different kinds of semiconductor photocatalysts can enhances its photocatalytic efficiency by increasing the charge separation. More recently, improved photocatalytic activity was reached by modifying TiO_2 particles with other oxides (such as Cr_xO_y, Fe_xO_y, V_xO_y, MoO_x, WO_x, etc.)

Hua Tian, et al., (2008) has investigated nanosized W-doped TiO_2 photocatalysts were synthesized by hydrothermal method. The photocatalytic activity of the undoped TiO_2 and W-doped TiO_2 photocatalysts was evaluated by the photocatalytic oxidation degradation of methyl orange in aqueous solution. By the photocatalytic degradation of methyl orange, the effect of W contents and the synthetic temperature on the photocatalytic activity of products were investigated. The characterization of the prepared photocatalysts were determined by, X-ray diffraction (XRD), Energy dispersive X-ray spectroscopy (EDX), Transmission electron microscopy (TEM) and BET surface areas analyzer. The results show that the photocatalytic activity of W-doped TiO_2 photocatalysts is much higher than that of undoped TiO_2.

In recent years, according to other published literatures, WO_3-doped TiO_2 coating on other absorbent such as charcoal activated was selected as an adsorptive support. This also has been confirmed by (Sangchay, 2017). In this study, WO_3-doped TiO_2 coating on charcoal activated (CA) was prepared by microwave-assisted sol-gel method. The photocatalytic and antibacterial activities of WO_3-doped TiO_2 coating on charcoal activated were examined by means of degradation of a methylene blue (MB) solution and the bacteria E.coli, respectively. The samples were characterized by XRD, EDS, and SEM. The results show that the concentration of WO_3 has an effect on hindrance of anatase growth, resulting in reduction photocatalytic and an antibacterial activity of WO_3-doped TiO_2 coated CA compared to that of pure TiO_2.

Therefore, many experiments have been performed to examine the ability of the semiconductor photocatalysts to promote the degradation and total mineralization of various pollutants. Typically, (Michalow, et al, 2008) proposed the tungsten-doped

titanium dioxide nanopowders within a various dopant concentration by one-step flame spray method. Extensive research has been performed to inspect the ability of the semiconductor photocatalysts to promote the degradation and total mineralization of various pollutants.

The photocatalytic activity of the powders was examined by the degradation of methylene blue (MB) and methyl orange (MO) in aqueous suspensions under UV-A (365 nm) as well as visible (400-500 nm) irradiation. The results were characterized by XRD, BET and TEM. In W-doped TiO_2 nanocomposite, the electrons can be more easily excited to the conduction band, simultaneously the free electrons are trapped on the surface by the W, and holes can react with the hydroxyl groups on the surface of the photocatalyst to create the hydroxyl radicals. In this syudy, in comparison to pure TiO_2, improved photocatalytic activity of the W-doped TiO_2 particles has been observed for the photodecolorization of methylene blue (MB) and methyl orange (MO).

All of the above results have been confirmed by (Paramasivam, et al, 2010). The study was demonstrated a very strong effect of tungsten addition to the TiO_2 nanotubes in terms of their photocatalytic activity. The photocatalytic activity for the different WO_3 contents was then investigated by decomposition measurements of an organic dye (Rhodamine B, RhB). SEM, EDX and XRD were used to investigate the characterization. In this study, the result show that the beneficial effect of WO_3 addition for the photocatalytic activity of TiO_2 nanotube layers both in UV and the visible region.

CHAPTER III

RESEARCH METHODOLOGY

This chapter describes the experimental procedure employed in this work

1. Synthesis of WO_3
2. Synthesis of TiO_2
3. Synthesis of TiO_2/WO_3
4. Photocatalytic activity test of synthesized TiO_2 and TiO_2/WO_3 nanoparticles of methylene blue (MB) as model pollutant

Chemicals and reagents

In this work, the used chemicals and reagents are shown in Table 7.

Table 7 List of chemicals and reagents

Chemicals	**Formula**	**Source**
Sodium-tungstate Dehydrate	$Na_2WO_4 \cdot 2H_2O$	Loba Chemie, Thailand
Citric Acid	$C_6H_8O_7$	Ajax Finechem, Thailand
Ethylene Glycol	$C_2H_6O_2$	Ajax Finechem, Thailand
Hydrochloric Acid	HCl	Rci Labscan, Thailand
Titanium Isopropoxide	TTIP	Sigma-Aldrich, Thailand
Propanol	C_3H_8O	Rci Labscan, Thailand

Experimental processes

1. Synthesis of WO_3

Figure 11 is the procedure to synthesize WO_3 by precipitation method.

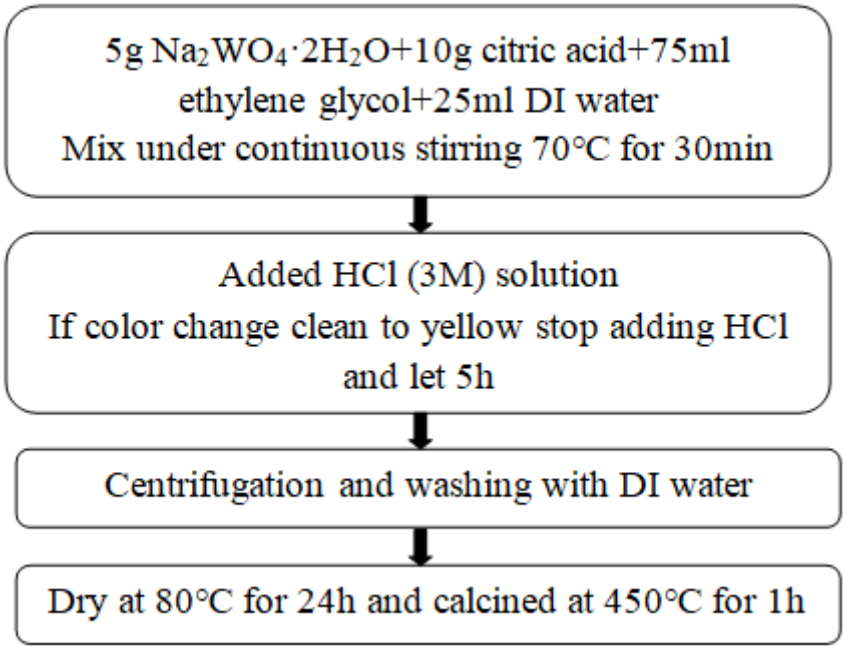

Figure 11 Procedure to synthesize WO_3

The detail of procedure as follows:

1. Sodium tungstate solution was prepared by dissolving 5g of sodium tungstate dehydrate ($Na_2WO_4 \cdot 2H_2O$) in the solvent mixture containing 10g citric acid, 75ml of ethylene glycol and 25ml of DI water at 70℃ with continuous stirring for about 30min.

2. HCl (3M) solution was added (to control the pH of the solution) to the above solution dropwise until the color change clean to yellow (under continuous stirring at 70℃). If change the color, stop adding HCl and let 5h leading to the precipitation of yellow-green WO_3 nanostructure.

3. After that, the precipitate was separated by centrifugation and wash with DI water five times to remove impure ions completely from the precipitate.

4. The resulting precipitate was dried at 80℃ for 24h and calcined at 450℃ for 1h.

2. Synthesis of TiO_2

The procedure to synthesize TiO_2, which is briefly summarized in Figure 12, involves the following steps:

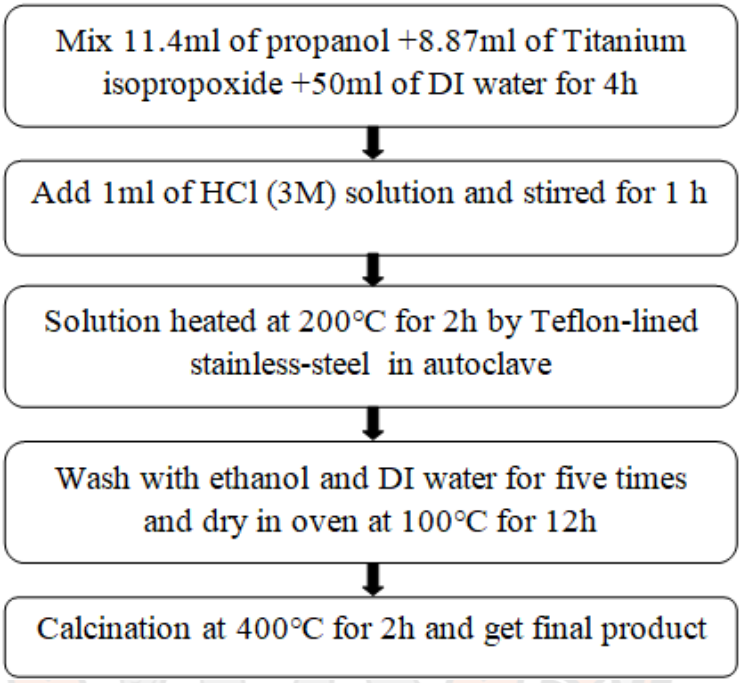

Figure 12 Procedure to synthesize TiO_2

The detail of procedure as follows:

1. 11.4ml of propanol and 8.87ml of Titanium isopropoxide (TTIP) were mixed in 50ml of DI water under stirring for 4h.

2. And then, 1ml of HCl (3M) solution was added to the above mixture and stirred for 1 h.

3. Then the mixture was transferred to the Teflon-lined stainless-steel autoclave and hydrothermally treated at 200℃ for 2h.

4. The resulting sample was recovered by centrifugation and washed with ethanol and DI water for five times then dried in oven at 100℃ for 12h.

5. After calcination at 400℃ for 2h, TiO_2 nanocomposite was achieved.

3. Synthesis of TiO_2/WO_3

The procedure to synthesize TiO2/WO3 is briefly summarized in Figure 13.

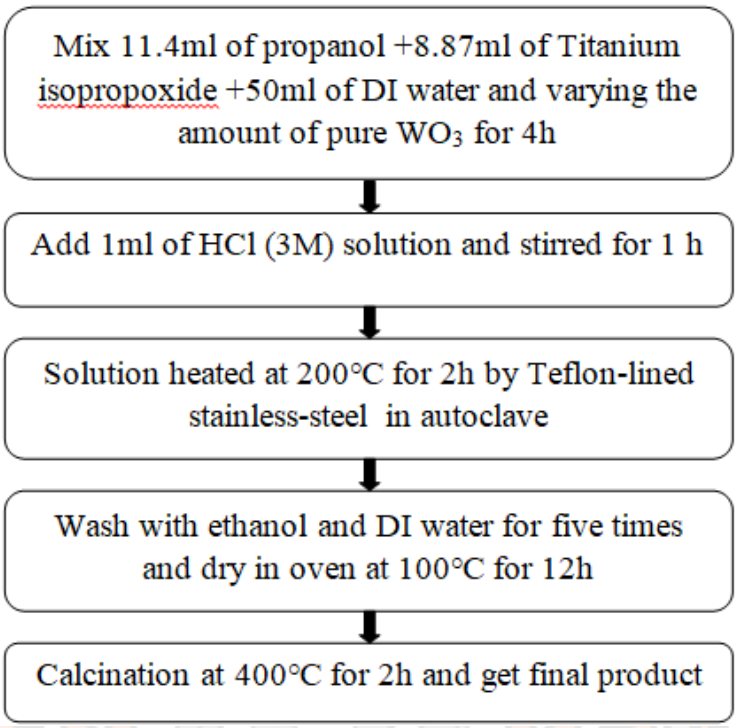

Figure 13 Procedure to synthesize TiO_2/WO_3

The detail of procedure as follows:

1. 11.4ml of propanol and 8.87ml of Titanium isopropoxide (TTIP) and varying the amount of pure WO_3 were mixed in 50ml of DI water under stirring for 4h.

2. And then, 1ml of HCl (3M) solution was added to the above mixture and stirred for 1 h.

3. Then the mixture was transferred to the Teflon-lined stainless-steel autoclave and hydrothermally treated at 200℃ for 2h.

4. The resulting sample was recovered by centrifugation and washed with ethanol and DI water for five times then dried in oven at 100℃ for 12h.

5. After calcination at 400℃ for 2h, TiO_2/WO_3 nanocomposite was achieved.

Table 8 Chemicals used in various WO_3 ratios of TiO_2/WO_3 nanocomposite

TiO_2/WO_3 %wt.	TTIP (g)	WO_3(g)
0	8.87	0
0.01	8.87	0.01
0.02	8.87	0.02
0.05	8.87	0.05
0.1	8.87	0.1
0.2	8.87	0.2
0.3	8.87	0.3

Characterization techniques

In this work, the techniques which were used for characterization of synthesized materials are shown in Table 9.

Table 9 Characterization of synthesized materials

Characterization techniques	Application
X-ray Diffraction (XRD)	Crystalline structure
Brunauer–Emmett–Teller (BET)	Specific surface area and pore size distribution
Transmission Electron Microscopy (TEM)	Surface morphology, crystallinity
UV-Vis Diffuse Reflection Spectroscopy (DRS)	Band gap energy
X-ray Photoelectron Spectroscopy (XPS)	Elemental composition, chemical state and electronic state of the elements within a material

Adsorption and photocatalytic activity tests

The organic removal efficiency of synthesized TiO_2/WO_3 was evaluated by using methylene blue (MB). For comparison, the adsorption and photocatalytic activity of pure TiO_2 and pure WO_3 was also tested. The procedure to evaluate the adsorption and photocatalytic activity of nanocomposite involved following steps:

1. 1×10^{-5}M (~3mg/L) of MB solution was prepared by DI water.
2. Added 0.05 g of TiO_2/WO_3 in 50 ml of the solution, and kept the solution in the dark condition for 30 min to reach adsorption-desorption equilibrium
3. The solution was irradiated by visible light under constant magnetic stirring.
4. The sample was collected every 5 min and centrifuged at 8,000 rpm for 10 min.
5. The sample was measured by UV-Vis absorption spectra (UV-6100 Double beam spectrophotometer)

The efficiency of MB removal and the rate constant (k) of photocatalytic degradation were calculated, as below equations:

$$\text{MB removal (\%)} = \frac{C_0 - C_t}{C_0} \times 100\% \quad (3.1)$$

where, C_0 is the initial concentration (mg/L) and C_t is the concentration at time t (mg/L)

$$\ln\left(\frac{c_0}{c_t}\right) = kt \quad (3.2)$$

where, C_0 is the initial concentration (mg/L), C_t is the concentration at time t (mg/L), k is first-order rate constant (min^{-1}) and t is time (min)

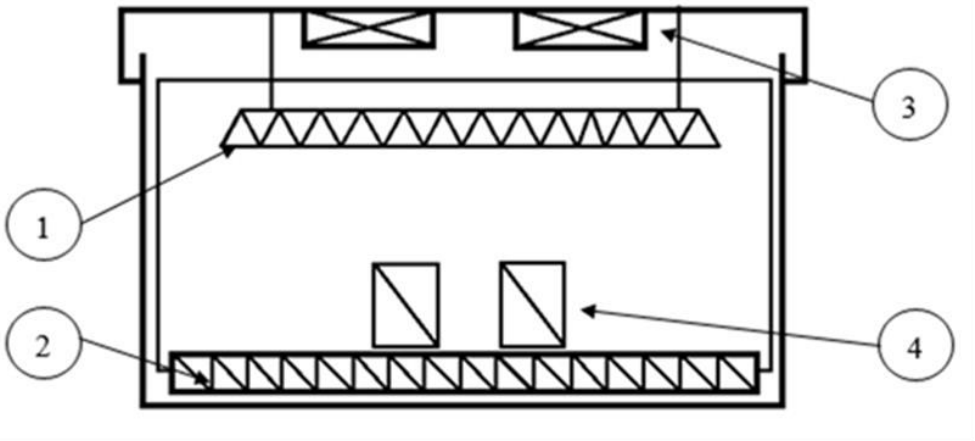

Figure 14 Photocatalytic activity test; 1. light source, 2. magnetic stirrer, 3. fans circulation and 4. beakers

CHAPTER IV

RESULTS AND DISCUSSION

Preliminary study

1. **Vary ratios of both TiO_2 and WO_3 in TiO_2/WO_3 nanocomposite**

In the preliminary study, both ratios of TiO_2 and WO_3 were varied to synthesize TiO_2/WO_3 nanocomposite. The ratios of TiO_2/WO_3 nanocomposite were following; $0.2TiO_2/0.8WO_3$, $0.4TiO_2/0.6WO_3$, $0.5TiO_2/0.5WO_3$, $0.6TiO_2/0.4WO_3$, and $0.8TiO_2/0.2WO_3$. The chemical reagents used for preparation is presented in Appendix. Pure TiO_2 was synthesized by hydrothermal method, whereas pure WO_3 and TiO_2/WO_3 nanocomposite were synthesized by precipitation method.

The adsorption and photocatalytic activity of nanocomposite was tested via methylene blue (MB) removal in the dark for 30 min and then under visible light and UV light irradiation for 120 min. The result of $0.2TiO_2/0.8WO_3$ is shown in Figures 15 and 16. The initial MB concentration of ~3 mg/L was effectively removed in the dark; the MB removal efficiency was approximately 94-97%. Since almost MB was removed by adsorption, the MB photocatalytic degradation under different irradiations was not observed. This revealed that the $0.2TiO_2/0.8WO_3$ performed the excellent adsorption ability and no photocatalytic activity under visible and UV light irradiation. This is because the WO_3 ratio in nanocomposite was too high, resulting in negative impact on MB photocatalytic degradation. Therefore, in the next experiment, the nanocomposite was synthesized by reducing WO_3 ratio from 0.4-0.8 to 0.01-0.3 and controlling the TiO_2 ratio as 1. In addition, the nanocomposite was synthesized by another method of hydrothermal. This is because the prior method of precipitation must exactly control the calcination temperature and pH. The solution was not changed to yellow-green color if small error of calcination temperature and pH was happened. Therefore, the hydrothermal method was easier to synthesize the nanocomposite.

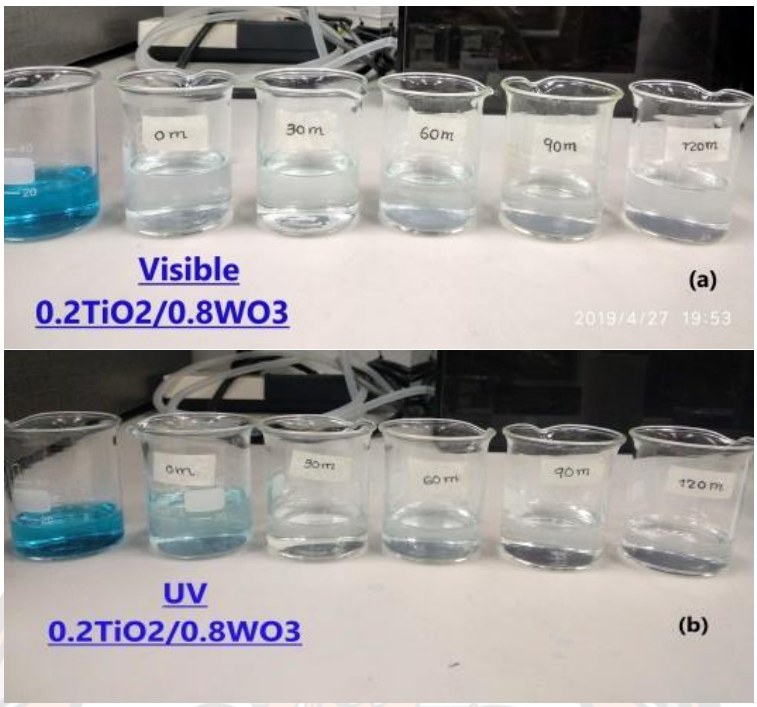

Figure 15 Methylene blue solution in the preliminary study

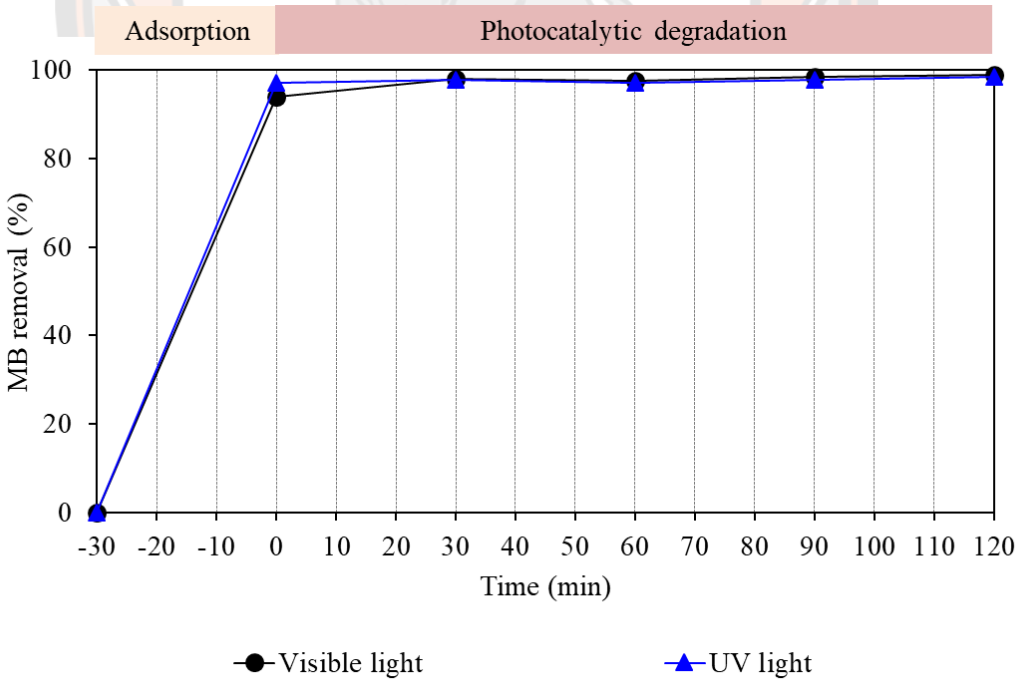

Figure 16 Methylene blue removal using $0.2TiO_2/0.8WO_3$ in the preliminary study

2. High calcination temperature

In this experiment, pure TiO_2 and pure WO_3 were synthesized by hydrothermal and precipitation methods respectively. However, TiO_2/WO_3 nanocomposite was synthesized by hydrothermal method and calcined at 620℃. The ratio of WO_3 in nanocomposite was following; 0.01, 0.02, 0.05, 0.1 and 0.2 %wt. Figure 17 illustrated phase composition of the nanocomposite; the rutile phase of TiO_2 was observed in the nanocomposite, and there was no anatase crystalline structure. The significant reason was that the anatase phase of TiO_2 was transformed to the rutile phase at 600℃. Although the anatase TiO_2 obtained the excellent photocatalytic activity for organic degradation, the rutile TiO_2 was not good photocatalyst. This is because the rutile phase caused a high electron-hole recombination rate, resulting in a low photocatalytic activity. Therefore, in the next experiment, the calcination temperature was changed to 400℃.

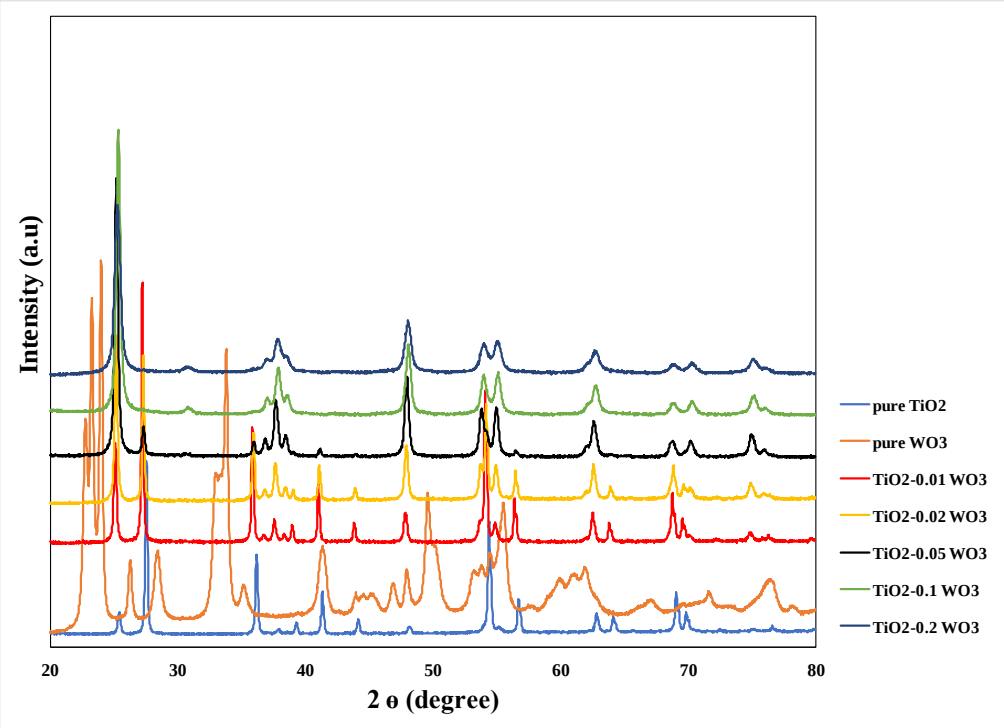

Figure 17 XRD patterns of TiO_2/WO_3 nanocomposite in the preliminary study

Characterization of synthesized nanocomposite

Finally, pure TiO_2 and TiO_2/WO_3 were synthesized by hydrothermal method and calcined at 400℃, while pure WO_3 was prepared by precipitation method. The phase composition was determined by X-Ray Diffraction (XRD) (Panalytical/Expert) with CuKα radiation at 1.54 Å. The XRD pattern was used to investigate the changes of phase structure of TiO_2 in nanocomposite prepared with different WO_3 ratios. Figure 18 displays the XRD patterns of TiO_2/WO_3 nanocomposite, pure TiO_2, and pure WO_3. The XRD patterns of pure TiO_2 was characterized by peaks at 2θ (JCPDS card No. 21-1272) as (101), (004), (200), (105), (118) and (215) planes of anatase crystal form. In the XRD patterns of WO_3, the planes corresponding to monoclinic phase of (020), (200), (112), (202), (222), (400), (420) and (622) was characterized by the peaks at 2θ (JCPDS card No. 89–4476) (Prabhu, et al., 2018). In the XRD patterns of TiO_2/WO_3 nanocomposite, the wider peaks were observed by increasing WO_3 ratios, because W^{6+} possibly combined into titania lattice and replaced Ti^{4+} to form W–O–Ti bonds (Ren, et al., 2011).

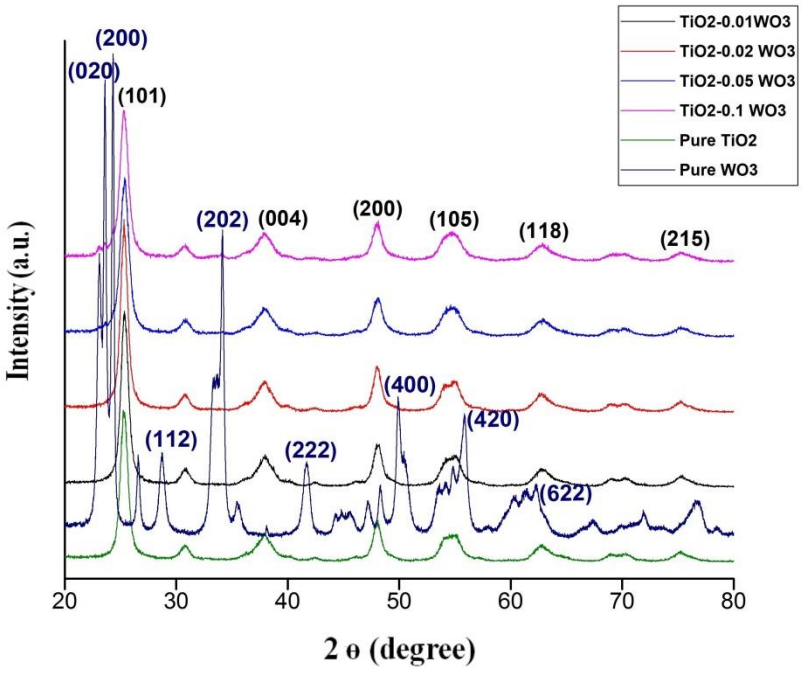

Figure 18 XRD patterns of pure TiO_2, pure WO_3 and TiO_2-WO_3 nanoparticles

Figure 19 shows the surface morphology by transmission electron microscopy (TEM). The TEM image of pure TiO_2 was agglomerated in spherical structure with average size of 100 nm (in Figure 19(e)), whereas pure WO_3 was rod-like structure with average size of 200 nm (as shown in Figure 19(f)). The morphology and their surface of TiO_2 becamed laced after adding small ratio of WO_3, because WO_3 acted as a support for TiO_2 crystal structure growth, as seen in TEM images of TiO_2/WO_3 nanocomposite.

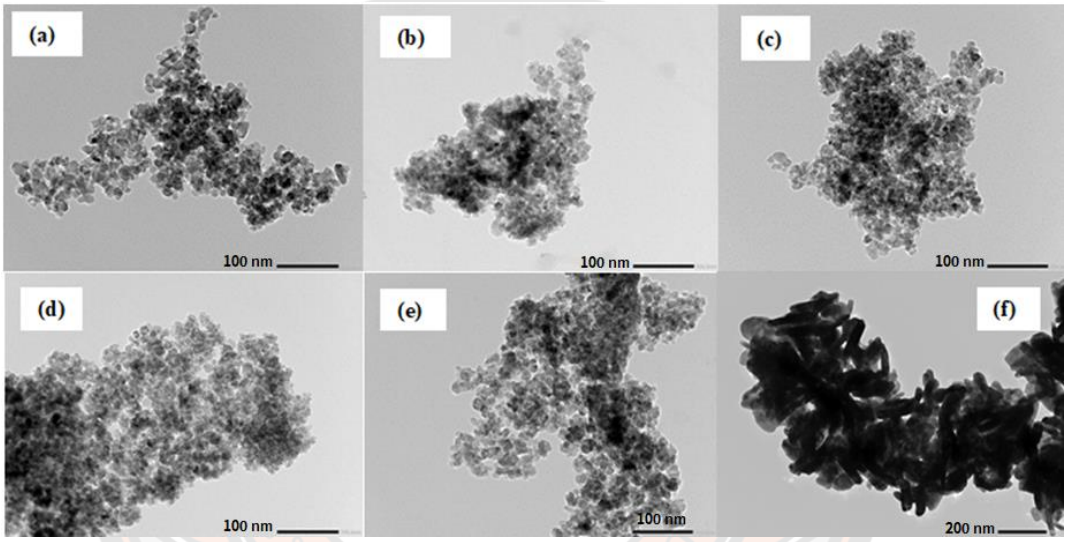

Figure 19 TEM images of (a) TiO_2-0.01WO_3, (b) TiO_2-0.02WO_3, (c) TiO_2-0.05WO_3, (d) TiO_2-0.1WO_3, (e) Pure TiO_2, and (f) Pure WO_3 nanoparticles

From the UV–Vis spectra in Figure 20 (a), the reflectance percentage of TiO_2/WO_3 heterostructure was decreased by increasing WO_3 ratios. The band gap was calculated by using Kubelka-Munk function, $[F(R)hv]^{1/2}$, ($F(R) = (1-R)^2/2R$), and R was the reflectance (Prabhu, et al., 2018). The results were presented in Figure 20 (b) and summarized in Table 10. The band gap of pure TiO_2 and pure WO_3 was 3.2eV and 2.6eV respectively as the same as theoretical value. The band gap of TiO_2 was decreased by adding small ratio of WO_3 as TiO_2/WO_3 nanocomposite; the band gap of 3.2ev for pure TiO_2 decreased to 3.0ev for TiO_2/WO_3 0.01%wt. and 2.8ev for TiO_2/WO_3 0.1%wt. The reduction in band gap was possibly from oxygen defects in the TiO_2 (by replacing oxygen atom in TiO_2). The lower band gap of TiO_2/WO_3

nanocomposite rather than pure TiO_2 caused that the nanocomposite can absorb visible light for organic photocatalytic degradation and achieves higher degradation efficiency (Prabhu, et al., 2018).

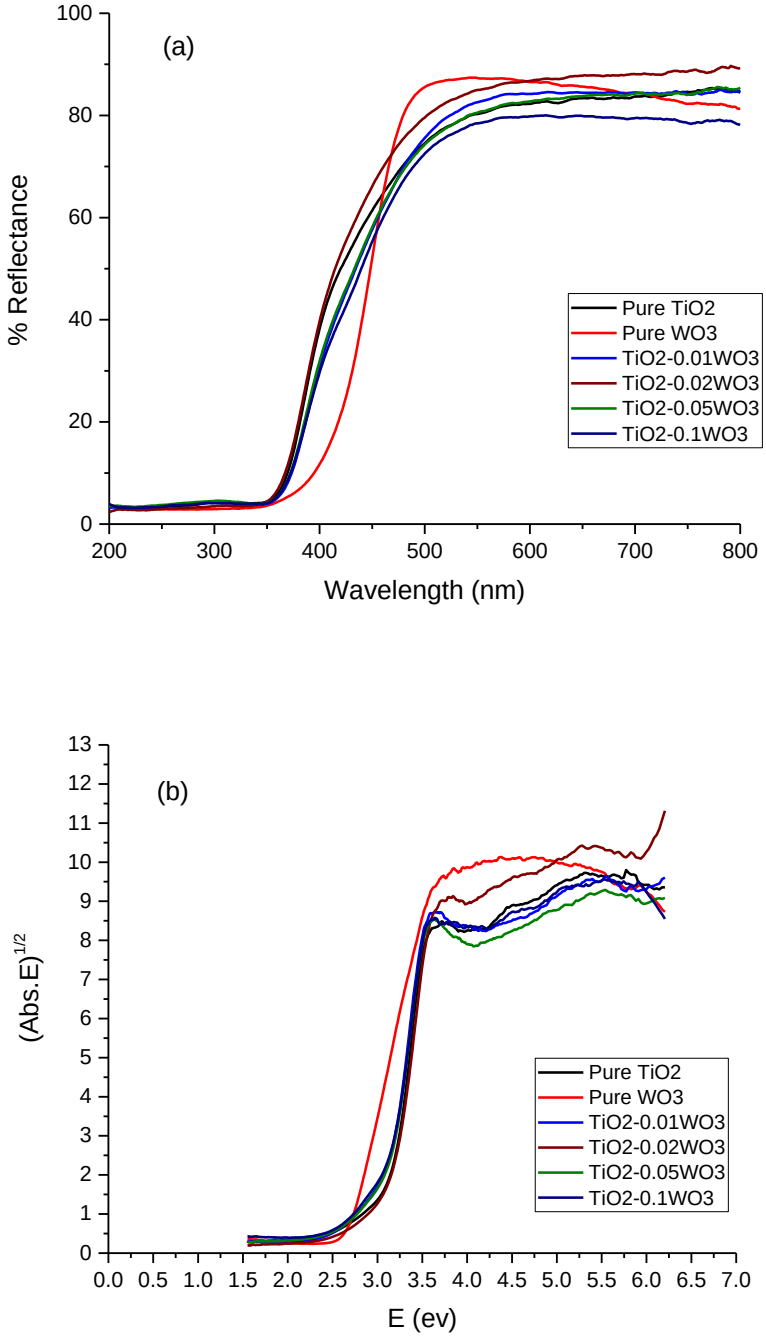

Figure 20 (a) UV–Vis spectra, and (b) band gap of TiO_2/WO_3 nanocomposite

Table 10 Band gaps of pure nanoparticles TiO_2-WO_3 nanoparticles

Sample	Band gap (eV)
Pure TiO_2	3.2
Pure WO_3	2.6
TiO_2-0.01WO_3	3.0
TiO_2-0.02 WO_3	3.0
TiO_2-0.05 WO_3	2.9
TiO_2-0.1 WO_3	2.8

The morphological property of pure TiO_2, pure WO_3, and TiO_2/WO_3 nanocomposite were analyzed using BET, and given in Table 11. The pure TiO_2 obtained the higher specific surface area and pore volume than pure WO_3, whereas the pore size of WO_3 was greater. For the TiO_2/WO_3 nanocomposite, the specific surface area and pore volume was increased by increasing WO_3 ratios; however, the pore size was decreasing. The nanocomposite containing large specific surface area can enhance the activity of organic photocatalytic degradation, due to high organic adsorption surface (Channei, et al., 2013).

Table 11 Surface properties of pure nanoparticles and TiO_2-WO_3 nanoparticles

Sample	Specific surface area (m^2/g)	Pore volume (cm^3/g)	Pore Size (Å)
Pure TiO_2	89.9167	0.2446	95.746
Pure WO_3	12.5430	0.0718	255.213
TiO_2-0.01wt%WO_3	71.0958	0.2412	122.569
TiO_2-0.02 wt%WO_3	96.0956	0.2448	90.631
TiO_2-0.05 wt%WO_3	101.1651	0.2461	89.472
TiO_2-0.1 wt%WO_3	105.6253	0.2550	79.571

The nanocomposite and pure TiO_2 were further analyzed by XPS technique, as shown in Figure 21. The specific XPS spectra were clarified in Figure 22; the peak was slightly shifted to the right when WO_3 was added. The more WO_3 was added, the more binding energy increased. These results supported the mixed structure of TiO_2 and WO_3 in the nanocomposite, resulting in the decreasing band gap of TiO_2/WO_3 nanocomposite. Furthermore, peaks of W-O (approximately 247eV) were clearly detected in TiO_2/WO_3 0.05%wt. and TiO_2/WO_3 0.1%wt.

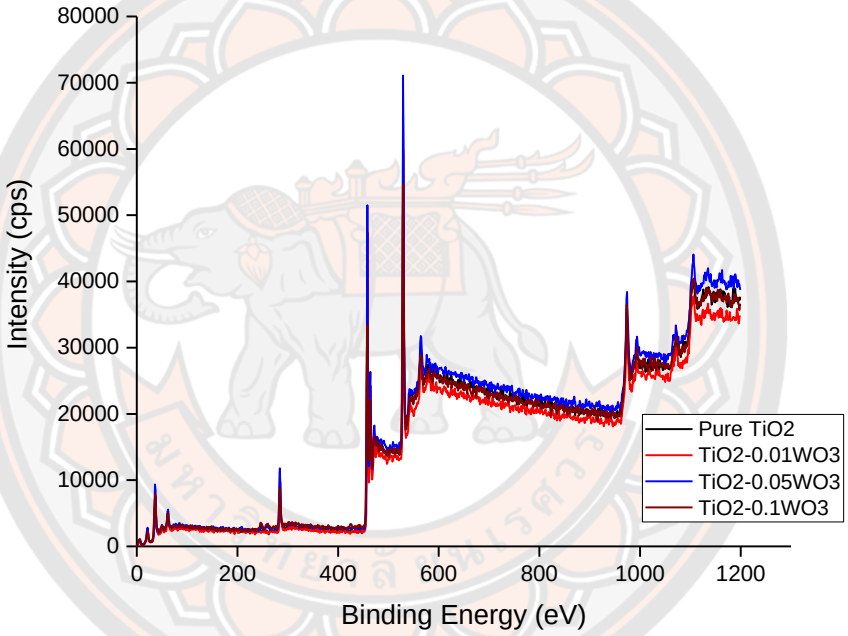

Figure 21 XPS spectra of TiO_2/WO_3 nanocomposite

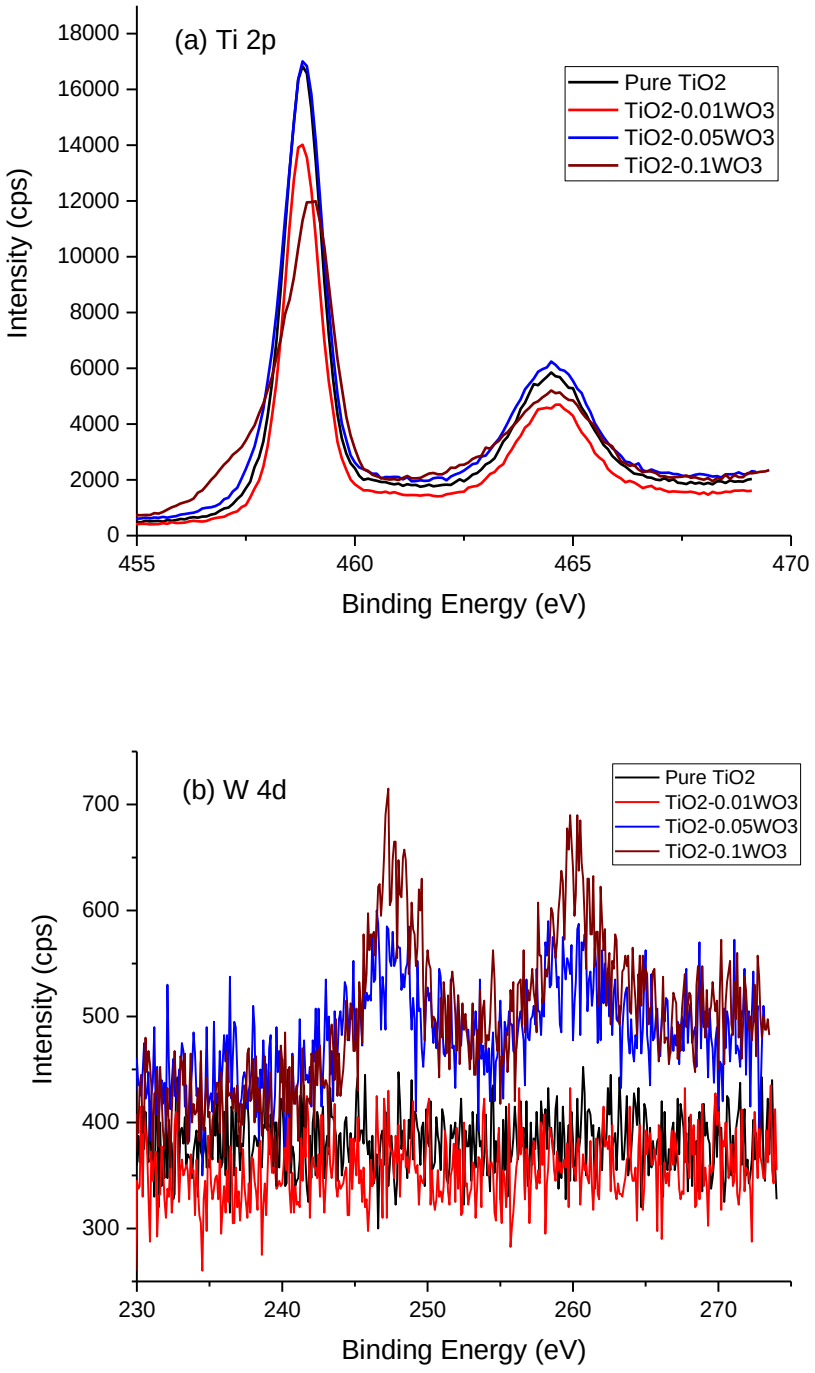

Figure 22 Specific XPS spectra of (a) Ti 2p and (b) W 4d of TiO_2/WO_3 nanocomposite

Photocatalytic degradation of methylene blue

The photocatalytic activity of TiO_2/WO_3 composite was investigated by methylene blue (MB) removal under visible light irradiation. The MB solution with TiO_2/WO_3 composite (as photocatalyst) was kept in the dark condition for 30 min to reach adsorption-desorption equilibrium and then irradiated under visible light for 60 min, as shown in Figure 23. For pure TiO_2, the MB removal efficiency was 19% in the dark and continuously increased to 35% in 10 min. These results revealed that partial MB was firstly removed by adsorption of TiO_2, later the MB was degraded by photocatalytic activity of TiO_2 until stable removal efficiency. Due to the wide band gap of TiO_2 (3.2 eV) and required UV for photocatalytic activation, the low removal efficiency of 32-35% was reached under visible irradiation in this study.

When WO_3 was added for preparing TiO_2/WO_3 nanocomposite, the addition effected on adsorption and photocatalytic activity of the nanocomposite. From Figure 24, the adsorption ability was increasing by WO_3 ratios; the adsorption ability was 22% for TiO_2/WO_3 0.01%wt. and it was increased to maximal value of 57% for TiO_2/WO_3 0.3%wt. which was the highest WO_3 addition ratio. However, pure WO_3 obtained excellent adsorption ability of 75%. The relationship of adsorption ability and WO_3 ratio in TiO_2/WO_3 nanocomposite was exponential relation (see in Figure 24). The results revealed that WO_3 was a photocatalyst which having good adsorption ability.

Since the initial MB concentration for photocatalytic degradation (t = 0) was different in each test of nanocomposite, first-order rate constant value (k) was used to identify the effect of WO_3 ratio on photocatalytic degradation. From Table 12, the k values of TiO_2/WO_3 0.01-0.02%wt. were similar as pure TiO_2 of approximately 0.02 min^{-1}. The explanation was that the WO_3 ratio was too low to obtain benefits from absorbing visible light for photocatalytic activation of nanocomposite. The k of photocatalytic degradation was significantly increased to 0.06 min^{-1} for TiO_2/WO_3 0.05%wt. and 0.08 min^{-1} for TiO_2/WO_3 0.1%wt. This demonstrated the sufficient WO_3 for absorbing visible and used it as light source to activate the photocatalytic activity in the nanocomposite.

At the high WO_3 of 0.2%wt. and 0.3%wt., the photocatalytic degradation was occurred very fast and reached stable MB removal efficiency in 5 min and the k value

was achieved of 0.27 and 0.33 min^{-1} respectively. According to this study, the increasing WO_3 ratios in TiO_2/WO_3 nanocomposite also enhance the photocatalytic activity. In contrast, very high adsorption of 75% and low k value of 0.02 min^{-1} was observed in pure WO_3. Therefore, the optimal WO_3 ratio was important concerning factor for synthesizing nanocomposite as visible-light-driven photocatalyst (Grbić, et al., 2014; Chai, et al., 2006). The intensive WO_3 ratio can cause the nanocomposite as excellent adsorbent with low photocatalytic activity. Moreover, the intensive WO_3 ratio increased the concentration of recombination centers, due to its small band gap. Later, the electron transport between the heterojunction formation of TiO_2 and WO_3 was reduced, and resulting in the decrease in photocatalytic activity.

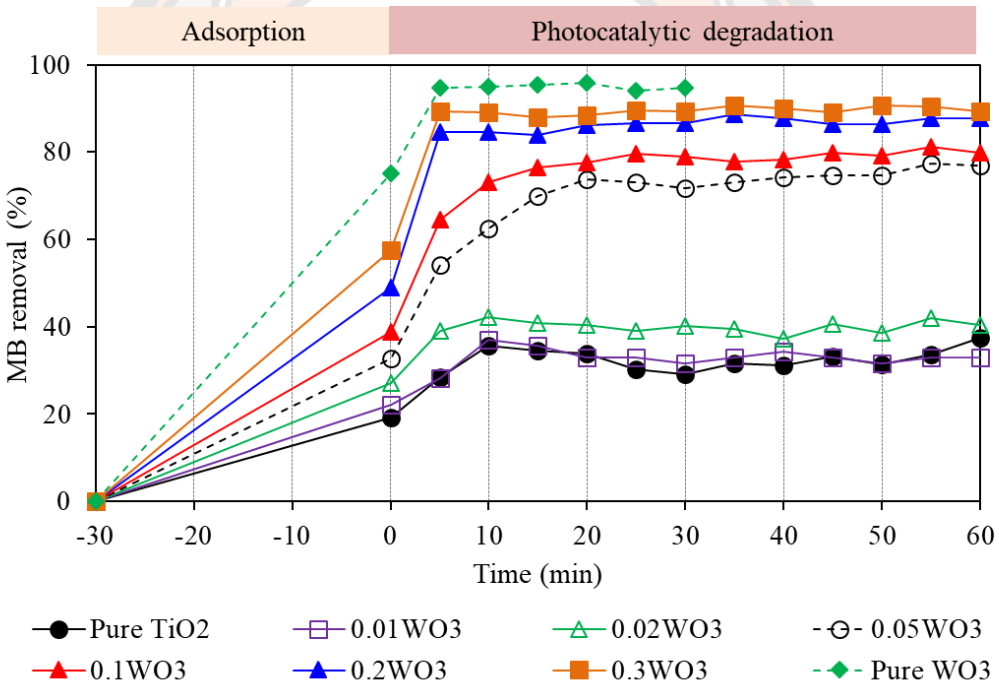

Figure 23 Methylene blue removal using TiO_2/WO_3 composite

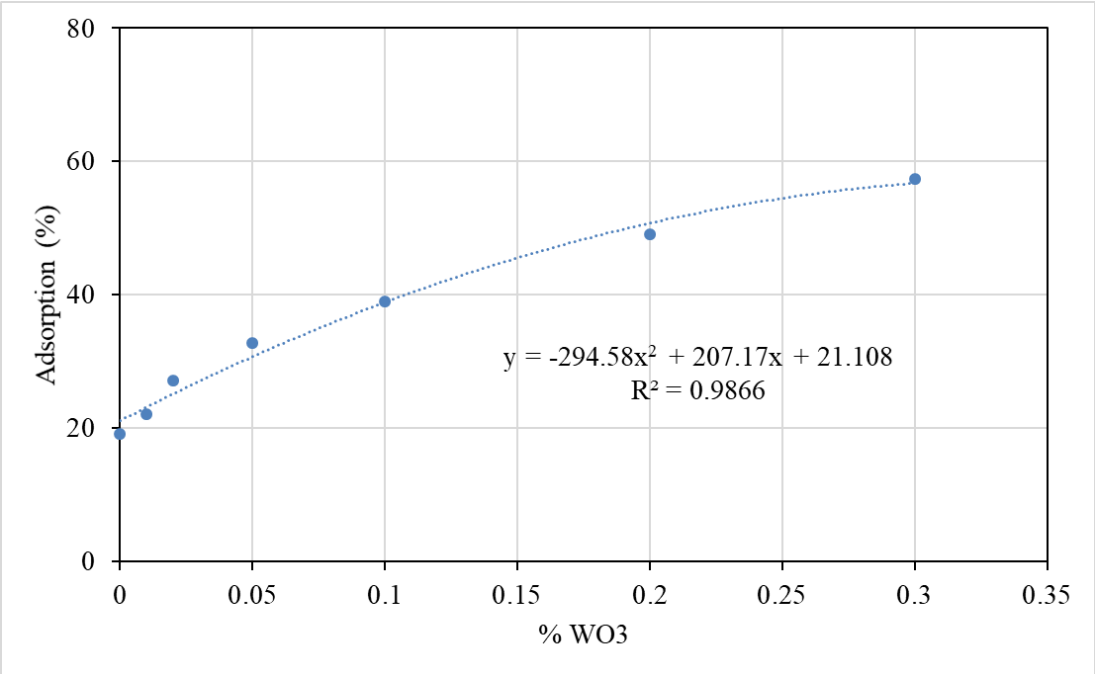

Figure 24 Methylene blue adsorption using TiO_2/WO_3 composite

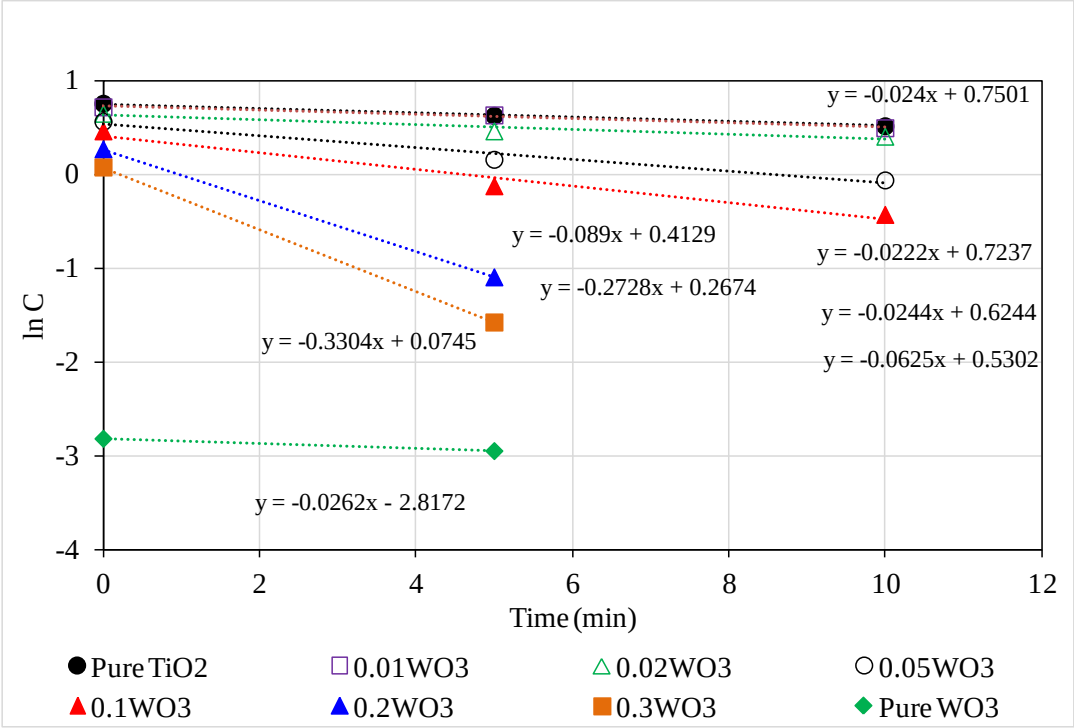

Figure 25 Methylene blue photocatalytic degradation using TiO_2/WO_3 composite

Table 12 Kinetic of methylene blue photocatalytic degradation using TiO_2/WO_3 composite

Sample	First-order rate constant value (k) (min^{-1})
Pure TiO_2	0.0240
Pure WO3	0.0262
TiO_2/WO_3 0.01%wt.	0.0220
TiO_2/WO_3 0.02%wt.	0.0244
TiO_2/WO_3 0.05%wt.	0.0625
TiO_2/WO_3 0.1%wt.	0.0890
TiO_2/WO_3 0.2%wt.	0.2728
TiO_2/WO_3 0.3%wt.	0.3304

The mechanism of MB photocatalytic degradation by TiO_2/WO_3 nanocomposite is illustrated in Figure 26. When the WO_3 was excited by visible light, holes (h^+) were formed in the valence band of WO_3 and transferred to the valence band of TiO_2. The electrons (e^-) in the conduction band of TiO_2 were transferred to the conduction band of WO_3 through the strong heterostructure, and then react with oxygen molecule (O_2). When e^- and h^+ reacted with redox species (i.e., H_2O and O_2), the active radicals of $^{\bullet}OH$ and $^{\bullet}O_2^-$ were formed. The $^{\bullet}OH$ were the key player to oxidize the adsorbed MB, and producing carbon dioxide gas (CO_2) and water (H_2O). Finally, the MB and other organic were removed from the wastewater (Chai, et al., 2006, Gao, et al., 2017).

$$^{\bullet}OH + MB \rightarrow \text{Photodegraded Products} \qquad (4.1)$$

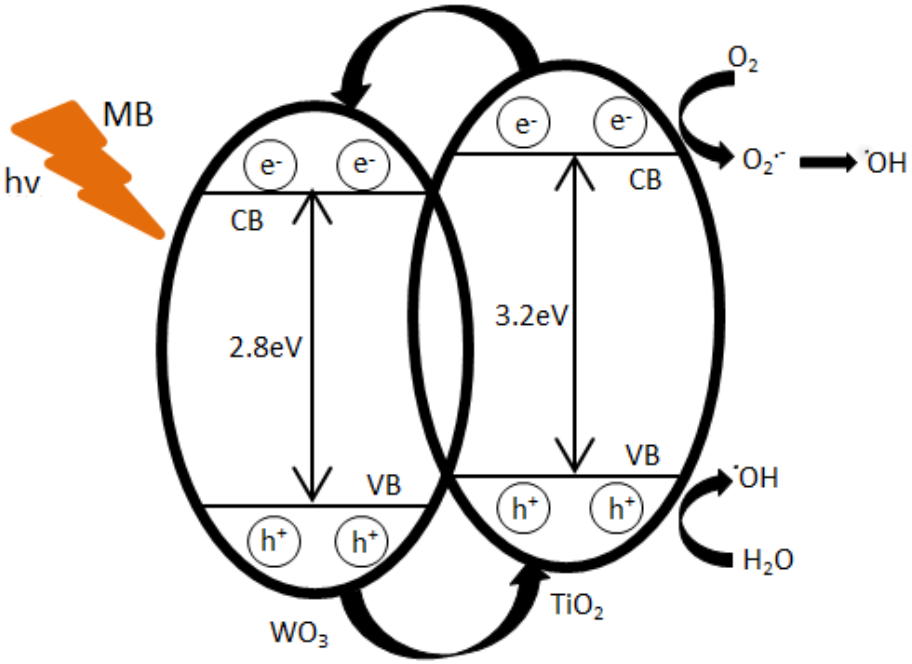

Figure 26 Photocatalytic degradation mechanism of methylene blue using TiO_2/WO_3 composite

CHAPTER V

CONCLUSION AND RECOMMENDATION

This chapter summarizes the main conclusions and reports for future work recommendations.

Conclusions

In this study, TiO_2 photocatalyst, which was requiring UV light for activation, was enhanced its organic photocatalytic degradation by adding WO_3. The peaks of anatase TiO_2 and monoclinic WO_3 was observed in the TiO_2/WO_3 nanocomposite. However, the characteristic of TiO_2/WO_3 nanocomposite was correlated to the WO_3 addition ratio; the band gap was decreased from 3.2eV for pure TiO_2 to 2.8eV for TiO_2/WO_3 0.1%wt., and the specific surface area was increased from 89.92 m^2/g for pure TiO_2 to 105.63 m^2/g for TiO_2/WO_3 0.1%wt. Both characteristics can enhance methylene blue (MB), as a model organic pollutant, photocatalytic degradation under visible light irradiation.

Two mechanisms of adsorption and photocatalytic degradation was occurred during MB removal. Approximately 20% MB was removed via adsorption by using pure TiO_2 and low WO_3 ratio of 0.01%wt., and their first-order rate constant (k) of photocatalytic degradation was only 0.02 min^{-1}. The MB adsorption ability and k value were increased by increasing WO_3 ratios. However, it should be noted that the intensive WO_3 ratio can cause the nanocomposite as excellent adsorbent with low photocatalytic activity. According to this study, the best photocatalytic degradation was found in TiO_2/WO_3 0.3%wt.; 57% MB was absorbed and later MB photocatalytic degradation was occurred with k value of 0.33 min^{-1}.

Recommendations

In this work, the TiO_2 adding with small ratio of WO_3 as nanocomposite was obtained the better photocatalytic activity rather than pure TiO_2 for MB degradation

and wastewater treatment. The following recommendation can be considered for further studies,

1. Synthesize TiO_2/WO_3 nanocomposite by other methods
2. Change calcination temperature and time to obtain the enhanced TiO_2/WO_3 nanocomposite as photocatalyst.
3. Test adsorption and photocatalytic degradation of TiO_2/WO_3 nanocomposite by using other organic pollutants and MB concentrations
4. Improve the photocatalytic activity of TiO_2/WO_3 nanocomposite by mixing with graphene-related materials

REFERENCES

REFERENCES

Afzali, A., Maghsoodlou, S., & Noroozi, B. (2018). Nanoporous Polymer/Carbon Nanotube Membrane Filtration: The “How-To” Guide to Computational Methods. In *Analytical Chemistry from Laboratory to Process Line* (pp. 99-150). Apple Academic Press.

Akpor, O. B., Ohiobor, G. O., & Olaolu, D. T. (2014). Heavy metal pollutants in wastewater effluents: sources, effects and remediation. *Advances in Bioscience and Bioengineering*, *2*(4), 37-43.

Ambulkar, A. R. (2017). Nutrient pollution and wastewater treatment systems. In *Oxford Research Encyclopedia of Environmental Science*.

Asiri, A. M., Al-Amoudi, M. S., Al-Talhi, T. A., & Al-Talhi, A. D. (2011). Degradation of Rhodamine 6G and phenol red by nanosized TiO_2 under solar irradiation. *Journal of Saudi Chemical Society*, *15*(2), 121-128.

Baker, R. W. (2012). *Membrane technology and applications*. John Wiley & Sons.

Böhmelt, T., Bernauer, T., Buhaug, H., Gleditsch, N. P., Tribaldos, T., & Wischnath, G. (2014). Demand, supply, and restraint: determinants of domestic water conflict and cooperation. *Global Environmental Change*, *29*, 337-348.

Cabral, J. P. (2010). Water microbiology. Bacterial pathogens and water. *International journal of environmental research and public health*, *7*(10), 3657-3703.

CDM Smith Inc. (2012). Guidelines for Water Reuse. Retrieved July 15, 2015, from http://nepis.epa.gov/-Adobe/PDF/P100FS7K.pdf.

Chai, S. Y., Kim, Y. J., & Lee, W. I. (2006). Photocatalytic WO_3/TiO_2 nanocomposite working under visible light. *Journal of electroceramics*, *17*(2-4), 909-912.

Chan, S. H. S., Yeong Wu, T., Juan, J. C., & Teh, C. Y. (2011). Recent developments of metal oxide semiconductors as photocatalysts in advanced oxidation processes (AOPs) for treatment of dye waste-water. *Journal of Chemical Technology & Biotechnology*, *86*(9), 1130-1158.

Channei, D., Inceesungvorn, B., Wetchakun, N., & Phanichphant, S. (2013). Kinetics study of photocatalytic activity of flame-made unloaded and Fe-loaded CeO2 nanocomposite. *International Journal of Photoenergy*, *2013*.

Cosgrove, W. J., & Rijsberman, F. R. (2014). *World water vision: making water everybody's business*. Routledge.

De la Cruz, N., Dantas, R. F., Giménez, J., & Esplugas, S. (2013). Photolysis and TiO_2 photocatalysis of the pharmaceutical propranolol: solar and artificial light. *Applied Catalysis B: Environmental*, *130*, 249-256.

Deblonde, T., Cossu-Leguille, C., & Hartemann, P. (2011). Emerging pollutants in wastewater: a review of the literature. *International journal of hygiene and environmental health*, *214*(6), 442-448.

Drinan, J. E., & Spellman, F. (2012). *Water and wastewater treatment: A guide for the nonengineering professional*. Crc Press.

Gaikwad, P. N., Wandre, T. M., Garadkar, K. M., Hankare, P. P., & Sasikala, R. (2016). Improvement of photocatalytic activity of TiO_2/WO_3 nanocomposite by the anionically substituted N and S. *Colloids and Surfaces A: Physicochemical and Engineering Aspects*, *506*, 804-811.

Gao, L., Gan, W., Qiu, Z., Zhan, X., Qiang, T., & Li, J. (2017). Preparation of heterostructured WO_3/TiO_2 catalysts from wood fibers and its versatile degradation abilities. *Scientific reports*, *7*(1), 1-13.

Gao, Y., Wang, H., Wu, J., Zhao, R., Lu, Y., & Xin, B. (2014). Controlled facile synthesis and photocatalytic activity of ultrafine high crystallinity TiO_2 nanocrystals with tunable anatase/rutile ratios. *Applied Surface Science*, *294*, 36-41.

Gonawala, K. H., & Mehta, M. J. (2014). Removal of color from different dye wastewater by using ferric oxide as an adsorbent. *Int J Eng Res Appl*, *4*(5), 102-109.

Gray, N. (2017). *Water technology*. CRC Press.

Grbić, B., Radić, N., Stojadinović, S., Vasilić, R., Dohčević-Mitrović, Z., Šaponjić, Z., & Stefanov, P. (2014). TiO_2/WO_3 photocatalytic composite coatings prepared by spray pyrolysis. *Surface and Coatings Technology*, *258*, 763-771.

Guo, J., Li, Y., Zhu, S., Chen, Z., Liu, Q., Zhang, D., ... & Song, D. M. (2012). Synthesis of WO_3@ Graphene composite for enhanced photocatalytic oxygen evolution from water. *Rsc Advances*, *2*(4), 1356-1363.

Hao, X., Li, M., Zhang, L., Wang, K., & Liu, C. (2017). Photocatalyst TiO_2/WO_3/GO nano-composite with high efficient photocatalytic performance for BPA degradation under visible light and solar light illumination. *Journal of industrial and engineering chemistry*, *55*, 140-148.

Hawari, A., Ramadan, H., Abu-Reesh, I., & Ouederni, M. (2015). A comparative study of the treatment of ethylene plant spent caustic by neutralization and classical and advanced oxidation. *Journal of environmental management*, *151*, 105-112.

Hezbullah, M., Sultana, S., Chakraborty, S. R., & Patwary, M. I. (2016). Heavy metal contamination of food in a developing country like Bangladesh: An emerging threat to food safety. *J Toxicol Environ Health Sci*, *8*(1), 1-5.

Hilal, N., Al-Zoubi, H., Darwish, N. A., Mohamma, A. W., & Arabi, M. A. (2004). A comprehensive review of nanofiltration membranes: Treatment, pretreatment, modelling, and atomic force microscopy. *Desalination*, *170*(3), 281-308.

Hinrichsen, D., & Tacio, H. (2002). The coming freshwater crisis is already here. *The linkages between population and water. Washington, DC: Woodrow Wilson International Center for Scholars*, 1-26.

Hu, X., Xu, P., Gong, H., & Yin, G. (2018). Synthesis and characterization of WO_3/Graphene nanocomposites for enhanced photocatalytic activities by one-step in-situ hydrothermal reaction. *Materials*, *11*(1), 147.

Jiang, L., Wang, Y., & Feng, C. (2012). Application of photocatalytic technology in environmental safety. *Procedia Engineering*, *45*, 993-997.

Kabcum, S., Kotchasak, N., Channei, D., Tuantranont, A., Wisitsoraat, A., Phanichphant, S., & Liewhiran, C. (2017). Highly sensitive and selective NO_2 sensor based on Au-impregnated WO_3 nanorods. *Sensors and Actuators B: Chemical*, *252*, 523-536.

Khataee, A. R., Zarei, M., & Ordikhani-Seyedlar, R. (2011). Heterogeneous photocatalysis of a dye solution using supported TiO_2 nanocomposite combined with homogeneous photoelectrochemical process: Molecular

degradation products. *Journal of Molecular Catalysis A: Chemical*, *338*(1-2), 84-91.

Le, H. A., Chin, S., & Jurng, J. (2012). Photocatalytic degradation of methylene blue by a combination of TiO_2-anatase and coconut shell activated carbon. *Powder Technology*, *225*, 167-175.

Lee, S. Y., & Park, S. J. (2013). TiO_2 photocatalyst for water treatment applications. *Journal of Industrial and Engineering Chemistry*, *19*(6), 1761-1769.

Lei, J. H., Alvarado, J. A., Li, H., Zhu, X. L., Tian, Y., & Liang, L. H. (2018, October). The advanced oxidation processes of oilfield wastewater: A review. In *IOP Conference Series: Earth and Environmental Science* (Vol. 191, No. 1, p. 012098). IOP Publishing.

Luis, A. M., Neves, M. C., Mendonça, M. H., & Monteiro, O. C. (2011). Influence of calcination parameters on the TiO_2 photocatalytic properties. *Materials Chemistry and Physics*, *125*(1-2), 20-25.

Mascolo, G., Comparelli, R., Curri, M. L., Lovecchio, G., Lopez, A., & Agostiano, A. (2007). Photocatalytic degradation of methyl red by TiO_2: Comparison of the efficiency of immobilized nanocomposite versus conventional suspended catalyst. *Journal of Hazardous Materials*, *142*(1-2), 130-137.

Mehmood, F., Iqbal, J., Jan, T., & Mansoor, Q. (2017). Structural, Raman and photoluminescence properties of Fe doped WO_3 nanoplates with anti cancer and visible light driven photocatalytic activities. *Journal of Alloys and Compounds*, *728*, 1329-1337.

Mekonnen, M. M., & Hoekstra, A. Y. (2016). Four billion people facing severe water scarcity. *Science advances*, *2*(2), e1500323.

Michalow, K. A., Vital, A., Heel, A., Graule, T., Reifler, F. A., Ritter, A., ... & Rekas, M. (2008). Photocatalytic activity of W-doped TiO_2 nanopowders. *Journal of Advanced Oxidation Technologies*, *11*(1), 56-64.

Naeem, K., & Ouyang, F. (2013). Influence of supports on photocatalytic degradation of phenol and 4-chlorophenol in aqueous suspensions of titanium dioxide. *Journal of Environmental Sciences*, *25*(2), 399-404.

Nakata, K., & Fujishima, A. (2012). TiO_2 photocatalysis: Design and applications. *Journal of photochemistry and photobiology C: Photochemistry Reviews*, *13*(3), 169-189.

Noble, R. D., & Stern, S. A. (Eds.). (1995). *Membrane separations technology: principles and applications*. Elsevier.

Ola, O., & Maroto-Valer, M. M. (2015). Review of material design and reactor engineering on TiO_2 photocatalysis for CO_2 reduction. *Journal of Photochemistry and Photobiology C: Photochemistry Reviews*, *24*, 16-42.

Olaolu, D. T., Akpor, O. B., & Akor, C. O. (2014). Pollution indicators and pathogenic microorganisms in wastewater treatment: Implication on receiving water bodies. *International Journal of Environmental Protection and Policy*, *2*(6), 205-212.

Ollis, D. F., & Al-Ekabi, H. (1993). *Photocatalytic purification and treatment of water and air: proceedings of the 1st International Conference on TiO2 Photocatalytic Purification and Treatment of Water and Air, London, Ontario, Canada, 8-13 November, 1992*. Elsevier Science Ltd.

Paramasivam, I., Nah, Y. C., Das, C., Shrestha, N. K., & Schmuki, P. (2010). WO_3/TiO_2 nanotubes with strongly enhanced photocatalytic activity. *Chemistry–A European Journal*, *16*(30), 8993-8997.

Pelaez, M., Nolan, N. T., Pillai, S. C., Seery, M. K., Falaras, P., Kontos, A. G., ... & Entezari, M. H. (2012). A review on the visible light active titanium dioxide photocatalysts for environmental applications. *Applied Catalysis B: Environmental*, *125*, 331-349.

Prabhu, S., Cindrella, L., Kwon, O. J., & Mohanraju, K. (2018). Photoelectrochemical and photocatalytic activity of TiO_2/WO_3 heterostructures boosted by mutual interaction. *Materials Science in Semiconductor Processing*, *88*, 10-19.

Prabhu, S., Manikumar, S., Cindrella, L., & Kwon, O. J. (2018). Charge transfer and intrinsic electronic properties of rGO-WO_3 nanostructures for efficient photoelectrochemical and photocatalytic applications. *Materials Science in Semiconductor Processing*, *74*, 136-146.

Ramos-Delgado, N. A., Hinojosa-Reyes, L., Guzman-Mar, I. L., Gracia-Pinilla, M. A., & Hernández-Ramírez, A. (2013). Synthesis by sol–gel of WO_3/TiO_2 for

solar photocatalytic degradation of malathion pesticide. *Catalysis Today, 209*, 35-40.

Rao, M. C. (2013). Structure and properties of WO_3 thin films for electrochromic device application. *J. Non-Oxide Glasses*, *5*, 1-8.

Ren, G., Gao, Y., Yin, J., Xing, A., & HUITAO Liu, H. (2011). Synthesis of high-activity TiO/sub 2//WO/sub 3/photo catalyst via environmentally friendly and microwave assisted hydrothermal process. *Journal of the Chemical Society of Pakistan*, *33*(5), 666-670.

Rijsberman, F. R. (2006). Water scarcity: fact or fiction?. *Agricultural water management*, *80*(1-3), 5-22.

Sangchay, W. (2017). WO_3-doped TiO_2 coating on charcoal activated with increase photocatalytic and antibacterial properties synthesized by microwave-assisted sol-gel method. *Journal of Nanotechnology*, *2017*.

Semerjian, L., & Ayoub, G. M. (2003). High-pH–magnesium coagulation–flocculation in wastewater treatment. *Advances in Environmental Research*, *7*(2), 389-403.

Sirés, I., Brillas, E., Oturan, M. A., Rodrigo, M. A., & Panizza, M. (2014). Electrochemical advanced oxidation processes: today and tomorrow. A review. *Environmental Science and Pollution Research*, *21*(14), 8336-8367.

Skorb, E. V., Antonouskaya, L. I., Belyasova, N. A., Shchukin, D. G., Möhwald, H., & Sviridov, D. V. (2008). Antibacterial activity of thin-film photocatalysts based on metal-modified TiO_2 and TiO_2:In_2O_3 nanocomposite. *Applied Catalysis B: Environmental*, *84*(1-2), 94-99.

Smyth, J. R., & Bish, D. L. (1988). *Crystal structures and cation sites of the rock-forming minerals* (p. 332). Boston: Allen & Unwin.

Sridhar, S. (2013). *Intermittent Water Supplies: Where and Why They Are Currently Used and Why Their Future Use Should Be Curtailed* (Doctoral dissertation).

Stefanov, B. (2015). *Photocatalytic TiO_2 thin films for air cleaning: Effect of facet orientation, chemical functionalization, and reaction conditions* (Doctoral dissertation, Acta Universitatis Upsaliensis).

Tahir, M., Nabi, G., Rafique, M., & Khalid, N. (2017). Nanostructured-based WO photocatalysts: recent development, activity enhancement, perspectives and

applications for wastewater treatment. *International Journal of Environmental Science & Technology (IJEST)*, *14*(11).

Thiruvenkatachari, R., Vigneswaran, S., & Moon, I. S. (2008). A review on UV/TiO_2 photocatalytic oxidation process (Journal Review). *Korean Journal of Chemical Engineering*, *25*(1), 64-72.

Van Gerven, T., Mul, G., Moulijn, J., & Stankiewicz, A. (2007). A review of intensification of photocatalytic processes. *Chemical Engineering and Processing: Process Intensification*, *46*(9), 781-789.

Wang, J. L., & Xu, L. J. (2012). Advanced oxidation processes for wastewater treatment: formation of hydroxyl radical and application. *Critical reviews in environmental science and technology*, *42*(3), 251-325.

Wei, Q., Yang, D., Fan, M., & Harris, H. G. (2013). Applications of nanomaterial-based membranes in pollution control. *Critical reviews in environmental science and technology*, *43*(22), 2389-2438.

Wilson, J. M., Wang, Y., & VanBriesen, J. M. (2014). Sources of high total dissolved solids to drinking water supply in southwestern Pennsylvania. *Journal of Environmental Engineering*, *140*(5), B4014003.

Yajun, W., Kecheng, L. U., & Changgen, F. E. N. G. (2011). Photocatalytic degradation of methyl orange by polyoxometalates supported on yttrium-doped TiO_2. *Journal of Rare Earths*, *29*(9), 866-871.

Yuangpho, N., Le, S. T. T., Treerujiraphapong, T., Khanitchaidecha, W., & Nakaruk, A. (2015). Enhanced photocatalytic performance of TiO_2 particles via effect of anatase–rutile ratio. *Physica E: Low-dimensional Systems and Nanostructures*, *67*, 18-22.

Zainudin, N. F., Abdullah, A. Z., & Mohamed, A. R. (2010). Characteristics of supported nano-TiO_2/ZSM-5/silica gel (SNTZS): photocatalytic degradation of phenol. *Journal of hazardous materials*, *174*(1-3), 299-306.

Zhang, T. C., Surampalli, R. Y., Lai, K. C., Hu, Z., Tyagi, R. D., & Lo, I. M. (Eds.). (2009, May). Nanotechnologies for water environment applications. American Society of Civil Engineers.

Zheng, C., Zhao, L., Zhou, X., Fu, Z., & Li, A. (2013). Treatment technologies for organic wastewater. *Water Treatment*, *11*, 250-86.

APPENDIX

Table 13 List of chemicals and reagents in the preliminary study

TiO_2/WO_3	Sodium-tungstate Dehydrate (g)	TiO_2 (g)
$0.2TiO_2/0.8WO_3$	3.2985	0.1996
$0.4TiO_2/0.6WO_3$	2.4738	0.3993
$0.5TiO_2/0.5WO_3$	2.0450	0.4951
$0.6TiO_2/0.4WO_3$	1.6492	0.5989
$0.8TiO_2/0.2WO_3$	0.8246	0.7986

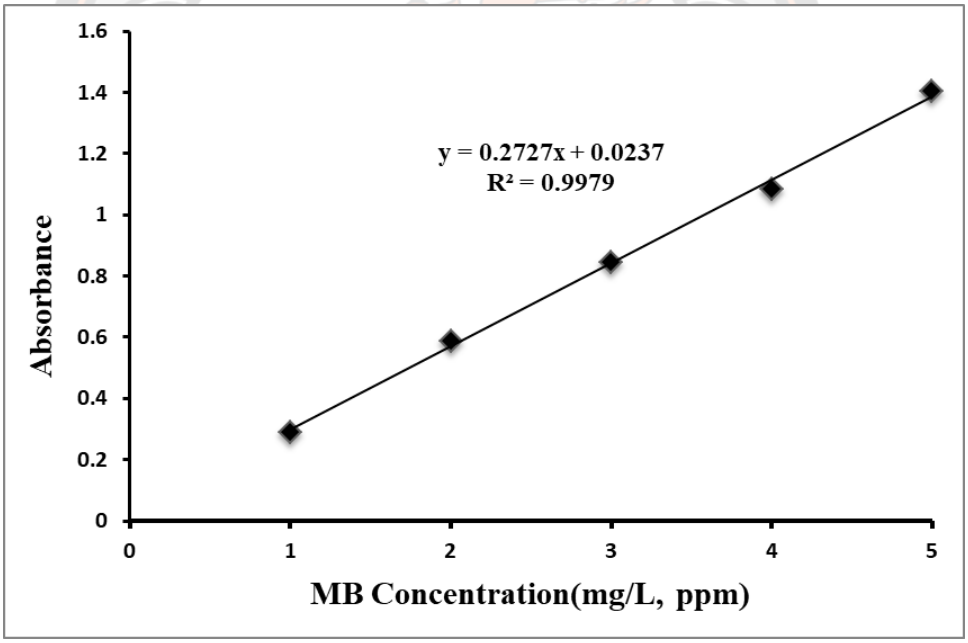

Figure 27 Calibration graph of MB

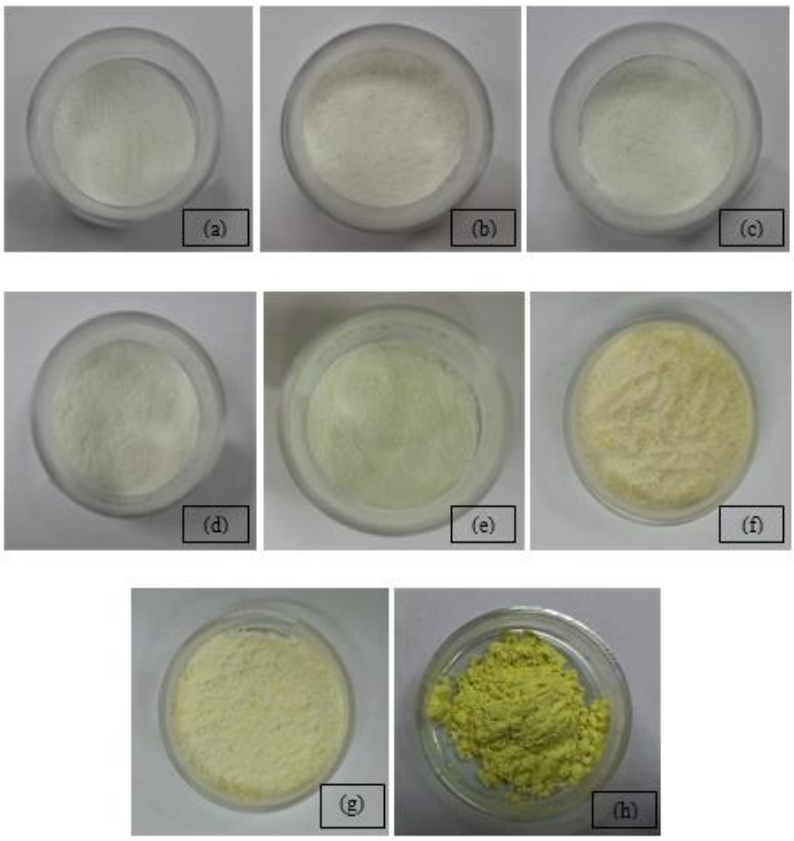

Figure 28 Photo of (a) pure TiO_2, (b) TiO_2/WO_3 0.01%wt., (c), TiO_2/WO_3 0.02%wt. (d) TiO_2/WO_3 0.05%wt., (e) TiO_2/WO_3 0.1%wt., (f) TiO_2/WO_3 0.2%wt., (g) TiO_2/WO_3 0.3%wt. and (h) pure WO_3